Affinity precipitation of proteins by surfactant-solubilized, ligand-modified phospholipids

ARTICLE *in* BIOTECHNOLOGY PROGRESS · SEPTEMBER 1992

Impact Factor: 2.15 · DOI: 10.1021/bp00017a011 · Source: PubMed

4 AUTHORS, INCLUDING:

Ruben G Carbonell
North Carolina State University
258 PUBLICATIONS **4,929** CITATIONS
SEE PROFILE

Peter K Kilpatrick
96 PUBLICATIONS **2,618** CITATIONS
SEE PROFILE

Affinity Precipitation of Proteins by Surfactant-Solubilized, Ligand-Modified Phospholipids

Daniel D. Powers, Betsy L. Willard, Ruben G. Carbonell, and Peter K. Kilpatrick*

Department of Chemical Engineering, North Carolina State University, Raleigh, North Carolina 27695-7905

The use of ligand-modified phospholipids solubilized in aqueous solution by nonionic surfactant for affinity precipitation of proteins is described. Avidin was precipitated by contact with solutions in which dimyristoylphosphatidylethanolamine (DMPE) functionalized with biotin (DMPE-B) was solubilized in octaethylene glycol mono-*n*-dodecyl ether ($C_{12}E_8$) solutions. The nonionic surfactant solubilizes the phospholipid in micelles above its critical micelle concentration (CMC) and in small submicellar aggregates below this concentration. At $C_{12}E_8$ concentrations significantly exceeding its CMC, determined to be about 100 μM, precipitation of avidin by solubilized DMPE-B is not observed. In this regime, binding of protein by DMPE-B was monitored by a hyperchroic shift in the protein's UV–visible spectrum at 231.5 nm. The data were analyzed using a model that considers the four binding sites on the protein to be independent and identical in binding strength for DMPE-B. Below the CMC of $C_{12}E_8$, precipitation is observed and is monitored by increasing turbidity of the solution. The kinetics of precipitation and the aggregate size measured by quasielastic light scattering were analyzed using Smoluchowski kinetics and the Mie scattering theory. These results help establish more completely the factors that influence the precipitation of proteins by ligand-modified phospholipids, and they are helpful in specifying conditions for the precipitation of other proteins.

Introduction

Precipitation, a commonly used purification step in schemes for isolating and recovering proteins from crude biological mixtures (Bell et al., 1983), is generally effected by addition of reagents, such as salts or cosolvents, which lower the solubility of the desired protein in aqueous solution. Addition of the solubility modifier results in a supersaturated solution of protein, in which seed particles form and then rapidly agglomerate due to interparticle attractions. This rapid agglomeration tends to be nonspecific, leading to entrainment of different biomolecules and, ultimately, an impure precipitate.

Recently, two affinity methods have been developed to impart greater selectivity to protein precipitation. In the first method (Larsson and Mosbach, 1979; Flygare et al., 1983; Larsson et al., 1984; Pearson et al., 1986; Van Dam et al., 1989), bivalent ligands (so-called homo-bifunctional ligands), which selectively bind to proteins possessing multiple binding sites, are used to cross-link the target molecule. This method has been used (Larsson and Mosbach, 1979; Flygare et al., 1983; Larsson et al., 1984) to purify oligomeric dehydrogenase enzymes with bifunctional NAD moieties, coupled together by a water-soluble spacer. At appropriate ratios of ligand to protein binding site, these ligand–protein complexes grow to a sufficiently large size to precipitate from solution. This method has also been used (Pearson et al., 1986) to selectively precipitate dehydrogenase enzymes with bifunctional triazine dye derivatives and to selectively precipitate proteins with surface histidine residues with bis-copper chelates (Van Dam et al., 1989). Flygare et al. (1983) and Larsson et al. (1984) point out that while this technique is specific and yields of greater than 90% of the desired protein can be obtained, there are a number of difficulties with the method. First, the ratio of ligand to protein must fall within a narrow range if high recovery is to be obtained. With low ligand-to-protein ratios, low yields are obtained because the ligand is exhausted before all of the protein has been bound. With high ligand-to-protein ratios, each desired protein molecule becomes completely bound with bifunctional ligand and there is no additional protein available for cross-linking. A second problem with the method is that at the optimum ligand-to-protein ratio the kinetics of precipitation seem to be very slow, taking as long as 20 h to precipitate yeast alcohol dehydrogenase with high recovery (Flygare et al., 1983). In the experiments with bis-copper chelates (Van Dam et al., 1989), precipitation was allowed to proceed for 48 h before recovery. A third problem with this type of affinity precipitation is that the formation of terminal aggregates which are not sufficiently large to precipitate is possible. For example, Flygare et al. (1983) found that with liver alcohol dehydrogenase, which is a two-subunit enzyme, precipitation could not be achieved because the bifunctional ligand simply cross-linked two protein molecules to form a dead-end dimer. Finally, the method is clearly limited to proteins with multiple binding sites.

An alternative affinity precipitation method uses so-called hetero-bifunctional ligands in which a portion of the precipitating molecule acts as an affinity ligand, while another group on the molecule can be used to effect the precipitation. Schneider et al. (1981) first exploited this idea by synthesizing a terpolymer of *N*-acryloyl-*p*-aminobenzoic acid, *N*-acryloyl-*m*-aminobenzamidine, and acrylamide and using it to selectively precipitate trypsin from mixtures of trypsin and chymotrypsin. The benzamidine group binds to the active site of trypsin while the benzoic acid group imparts solubility to the polymer above pH 6.0, a level at which the acid groups are mostly ionized. When the pH is reduced below 5.0, however, the acid group becomes protonated and the polymer solubility is greatly reduced. Yields of trypsin in excess of 75% with purities

8756-7938/92/3008-0436$03.00/0

greater than 90% were obtained. This technique has been subsequently used to purify trypsin with modified chitosan (Senstad and Mattiasson, 1989a), to purify protein A with IgG-modified hydroxypropylmethyl–cellulose acetate succinate (Taniguchi et al., 1989), and to purify wheat germ agglutinin with chitosan (Senstad and Mattiasson, 1989b). However, this method also has some drawbacks. First, the actual precipitation step requires a significant change in solution pH which is likely to induce the aggregation and precipitation of other proteins in the mixture. Second, in some cases, the synthesis of the modified polymer can be complex and expensive. Third, the high charge density on the polymer may lead to nonspecific adsorption of charged proteins and thus reduce the purity of the desired product protein obtained. In a variation on this latter type of affinity precipitation, Senstad and Mattiasson (1989c) have recently described the precipitation of lactate dehydrogenase with Blue Dextran. The protein–polymer complex was precipitated by cross-linking with concanavalin A rather than by changing solvent conditions. This method overcomes the disadvantages associated with the charged polymeric heterofunctional ligands, but it introduces an additional binding step in the process and significantly complicates the recovery of the ligand for reuse.

We have recently described (Guzman et al., 1990) a third type of affinity precipitation technique in which ligand-modified phospholipids that have been solubilized in aqueous solution by nonionic surfactants are contacted with protein molecules containing multiple binding sites. After binding to one of the target protein molecules, the phospholipid moieties apparently reduce the solubility of the protein in the aqueous phase, causing its precipitation. The hydrophobic tails of the lipid are likely to interact and lead to the formation of the agglomerates. A schematic illustration of this mechanism is shown in Figure 1. This interaction leads to growing complexes which ultimately precipitate from solution. The method was demonstrated by solubilizing dimyristoylphosphatidylethanolamine–biotin (DMPE-B) in aqueous solutions of octaethylene glycol mono-*n*-dodecyl ether ($C_{12}E_8$) and precipitating avidin from both simple protein mixtures and from egg white solutions, a crude source of avidin. The biotin moiety has high specificity for binding to avidin (Green, 1963), which is an oligomeric protein with four equivalent binding sites. Purities and yields of greater than 90% were obtained (Guzman et al., 1990). In similar experiments conducted with DMPE, i.e., phospholipid without the biotin functional group attached, there was no evidence of precipitation. The advantage of this method is that even though aggregation is induced by the specific interaction, which makes the method selective, there is no change required in solvent conditions. The protein bound to the lipid-modified ligand simply has a low solubility in aqueous solution. The method can potentially be applied to any protein for which a strong-binding ligand can be identified and covalently attached to a phospholipid.

Detailed studies of the mechanism and kinetics of phospholipid binding and protein precipitation are described here for the avidin–DMPE-B system. The binding of avidin to DMPE-B was studied at $C_{12}E_8$ concentrations both above and below its critical micelle concentration (CMC). At surfactant concentrations significantly exceeding the CMC, protein precipitation is not observed. In this region the binding of protein was measured using a hyperchroic shift in the protein's ultraviolet spectrum at 232 nm, and the data were analyzed using a model that considered all of the binding sites on the protein to be equal and independent. Thus, at concentrations of $C_{12}E_8$ well above the CMC, the protein can still bind to the solubilized ligand in the micelles, but the surfactant concentration is high enough to prevent any aggregation of ligand-bound protein. Below the CMC of $C_{12}E_8$, precipitation is observed by increased turbidity of the solution. It is apparent that, below the CMC, the ligand is solubilized in the form of submicellar aggregates. When specifically bound to the ligand, the solubility of the protein is modified temporarily due to the hydrophobic properties of DMPE-B, and precipitating aggregates are formed. The mechanism of interaction of the protein with the ligand is illustrated in Figure 1. The kinetics of precipitation, the yield of precipitation, and the aggregate size measured by quasielastic light scattering (QLS) were analyzed using Smoluchowski kinetics and the Mie scattering theory. These results establish more definitively the factors that influence the precipitation of proteins using ligand-modified phospholipids, and they are helpful in specifying conditions for the affinity precipitation of other proteins by this method.

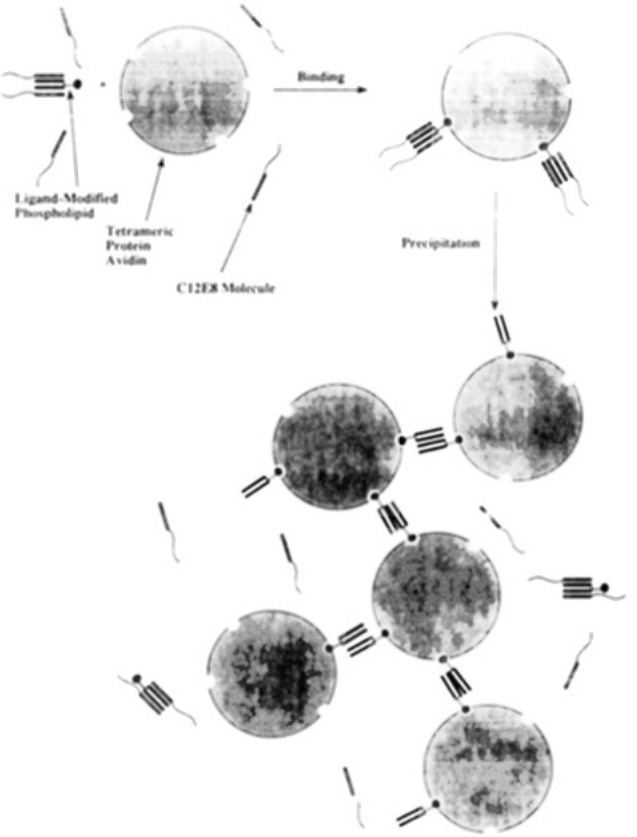

Figure 1. Schematic of affinity precipitation mechanism. Depiction of aggregation occurring via hydrophobic interaction between the nonpolar hydrocarbon tails of the biotinylated phospholipid, the head groups of which are bound to separate avidin molecules.

Experimental Section

Materials. Dimyristoyl-L-α-phosphatidylethanolamine (DMPE), dimyristoyl-L-α-phosphatidylcholine (DMPC), avidin, triethylamine, molybdenum blue reagent, and 4-(dimethylamino)cinnamaldehyde reagent were obtained from Sigma Chemical Co. (St. Louis, MO). Octaethylene glycol mono-*n*-dodecyl ether ($C_{12}E_8$) was purchased from Nikko Chemicals (Tokyo, Japan), and biotinyl-*N*-hydroxysuccinimide ester (biotin-NHS) was from Pierce (Rockford, IL). All chemicals were the highest purity available and were used without further purification.

Mallinckrodt AR ammonium carbonate and all solvents (HPLC grade) were obtained from Fisher Scientific Co. (Raleigh, NC). Deionized water was obtained by passage through a Barnstead Nanopure System (Newton, MA). Whatman high-performance thin-layer chromatography (HPTLC) silica gel plates were obtained from American Scientific Products (Charlotte, NC). Buffer used for all solution preparations and dilutions was 0.2 M ammonium carbonate, pH 8.9 (stock buffer).

Synthesis of Biotinylated Phospholipid. Biotin was covalently attached to DMPE following the protocol described by Bayer et al. (1979) as modified by Powers et al. (1989). Biotin-NHS was used to obtain dimyristoyl-L-α-phosphatidylethanolamine biotin (DMPE-B) shown below. The purity of the product was determined by

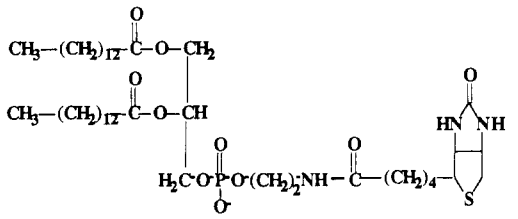

spotting HPTLC plates with identical samples of product and starting materials. The plates were developed simultaneously in the same chamber with $CHCl_3$:CH_3OH:H_2O (80:25:2 v/v); some plates were sprayed with molybdate blue reagent to visualize phosphate-containing phospholipid and the others with 4-(dimethylamino)-cinnamaldehyde reagent (McCormick and Roth, 1970) to visualize the biotin-containing species. Each product gave a single spot that migrated differently from the biotin-NHS or the DMPE standards when analyzed in this way. Purity of the ligand-modified phospholipids was also assessed by titrating standard avidin solutions with either micellar solutions of the phospholipid or with aliquots of the phospholipid incubated with 0.1 M NaOH as described below. The purity of DMPE-B was judged to be greater than 90% by this method.

Solubilization of Phospholipid in Surfactant Solutions. Test solutions of biotin-containing phospholipid in $C_{12}E_8$ were prepared by adding sufficient DMPE-B to solutions of $C_{12}E_8$ at concentrations varying from 100 μM to 50 mM to give a 2:1 (mol/mol) mixture of $C_{12}E_8$/phospholipid. These mixtures were then either heated with vigorous stirring for 40 min at 70–80 °C and allowed to stand overnight at room temperature or stirred vigorously overnight at room temperature. Mixtures prepared in either way were centrifuged in a bench-top centrifuge at 5000 rpm for 15 min. The supernatant was removed and filtered through a 0.2-μm membrane filter (Nalgene) in order to remove any remaining suspended DMPE-B. The DMPE-B concentration in the filtered supernatant was then measured by the hyperchroic shift titration method described below. Dilutions for use in other experiments were prepared from these test solutions. In cases for which the solutions were heated, significant subcooling occurred upon return to room temperature resulting in metastable micellar solutions. The phospholipid present in these metastable solutions was observed to remain solubilized for periods of days before finally precipitating from solution, and measurements of micelle size and affinity precipitation with metastable solutions were possible.

Critical Micelle Concentration Determination. Surface tension measurements were made at 25 °C on solutions of $C_{12}E_8$ and $C_{12}E_8$/DMPE-B (7.6:1 mol/mol). A Fisher Autotensiomat tensiometer was used with a platinum–iridium ring that had a mean circumference of 6 cm. Test solutions (0.001 M in $C_{12}E_8$) were successively diluted with standard buffer, and the surface tension of each was measured. Plots of surface tension as functions of $C_{12}E_8$ concentration were employed to determine the critical micelle concentration of each solution (Adamson, 1982).

Measurement of Micelle Sizes. Micellar aggregate sizes were determined at 25 °C by quasielastic light scattering (QLS) using an Innova 70 argon ion laser source (Coherent, Palo Alto, CA). Light was scattered from samples placed in a temperature-controlled, filtered toluene bath positioned in a BI-200 (Brookhaven) goniometer system. Scattered light was impinged on an EMI 9863/350 photomultiplier tube. The signal was analyzed by a BI-2030AT digital correlator having 128 real-time data channels or a BI-8000AT digital correlator having 128 real-time data channels and allowing geometric spacing of sample times. Intensity-weighted mean diameters were obtained either by the method of cumulants (Koppel, 1972) or by the CONTIN size distribution analysis method (Provencher, 1982a,b).

Activity of Avidin. The biotin-binding capacity of avidin was determined at 25 °C using the spectrophotometric method of Green (1963). This method is based on the observed hyperchroic shift to the red in the ultraviolet spectrum of avidin in solution upon binding of biotin. With avidin (3.0 mL; 0.068 mg/mL) in the sample cuvette and standard buffer in the reference cuvette, the spectrophotometer was electronically zeroed. Aliquots of d-biotin (0.049 mg/mL) in standard buffer were added to the sample cuvette until no further increase in absorbance occurred after three successive biotin additions. The equivalence point was determined from a plot of absorbance as a function of moles of added biotin. Either a Model UV-160 or Model UV-265 spectrophotometer (Shimadzu Corp., Kyoto, Japan) was used for these measurements.

Titration of Avidin to Determine Ligand-Modified Phospholipid Concentration. In order to determine the actual DMPE-B concentration in test solutions, we developed two titration methods. The first method was based on measurement of the hyperchroic shift of avidin bound to biotin-modified phospholipid in $C_{12}E_8$ solutions of sufficiently high concentration (1 mM) to prevent aggregation of the avidin. In this method, avidin (3.0 mL; 0.068 mg/mL), $C_{12}E_8$, and standard buffer were placed in the sample and reference cuvettes and the spectrophotometer was electronically zeroed. Aliquots of DMPE-B in standard buffer were added to the sample cuvette and buffer only was added to the reference cuvette, and absorbance at 231.5 nm (hyperchroic shift maximum for avidin/DMPE-B) was monitored until no further increase in absorbance occurred, usually 30–40 min per aliquot. This procedure was repeated until no absorbance increase was observed on addition of three successive aliquots of the titrant. The equivalence point was determined from a plot of absorbance vs volume of titrant. In the second method, an aliquot (100–500 μL) of the stock solution was incubated at room temperature overnight with sufficient 1 M NaOH to give a final concentration of 0.1 M NaOH in the mixture. Control experiments showed that biotin was completely cleaved from the biotinylated phospholipid, and the activity of biotin was not affected by these hydrolysis conditions. These reaction mixtures were then used to titrate previously standardized avidin in the usual manner with the exception that sufficient $C_{12}E_8$ was placed in the sample and reference cuvettes to give a 1 mM

concentration of $C_{12}E_8$. Either titration method gave the same result, but the hydrolysis method was much faster. It should be noted for future comparison to aggregation experiments that the magnitude of the hyperchroic shift measured in 1 μM avidin solutions never exceeded a value of 0.1 absorbance units.

Binding of DMPE-B in Micelles to Avidin. In order to determine the binding constant of micelle-solubilized DMPE-B to avidin, 1 μM avidin in 3.0 mL of standard buffer containing 1 mM $C_{12}E_8$ was placed in the sample and reference cuvettes of a spectrophotometer and zeroed. To the sample cuvette were added 10-μL aliquots of a DMPE-B solution (166 μM DMPE-B and 5 mM $C_{12}E_8$) and to the reference cell were added aliquots of buffer containing 5 mM $C_{12}E_8$. After the addition of each aliquot, the increase in absorbance at 231.5 nm was monitored until constant. In order to obtain sufficiently high concentrations of DMPE-B to observe the maximum obtainable absorbance, a more concentrated solution of DMPE-B (1.66 mM DMPE-B and 50 mM $C_{12}E_8$) was used for the final two aliquots. A correction was made for the small absorbance increase due to DMPE-B by subtracting the absorbance obtained from a control experiment in which aliquots of the stock DMPE-B solutions were added, under the same conditions, to a sample cuvette containing only buffer and $C_{12}E_8$.

Kinetic Measurements of Avidin Aggregation. Aggregation of avidin with biotinylated phospholipid was followed by monitoring absorbance values at 233 nm in a Shimadzu Model UV-265 spectrophotometer equipped with a temperature-controlled sample compartment maintained at 25 °C. As the aggregated complexes of avidin and bound phospholipid grow in size from a few hundred angstroms to several thousand angstroms, the solution becomes turbid and this is reflected in an increasing absorbance value. Avidin solution in standard buffer was placed in the sample cuvette, and the spectrophotometer was zeroed electronically with only standard buffer and an appropriate concentration of $C_{12}E_8$ in the reference cuvette. To initiate an experiment, biotinylated phospholipid solution was added to the reference and sample cuvette and absorbance values were recorded until a decrease was observed. The decrease in absorbance indicated that the precipitated protein aggregates had begun to settle giving a corresponding decrease in the turbidity of the solution. Two methods were employed to determine aggregate sizes by QLS using the instrumentation previously described: either (1) aliquots were removed from the spectrophotometer sample cuvette, immediately diluted 1 part to 100 parts with standard buffer, and reserved for later size measurements or (2) the biotinylated phospholipid was added to avidin in a QLS sample cell, the resulting mixture was immediately placed in the sample compartment of the BI-200, and size measurements were taken as aggregation proceeded.

Results and Discussion

The first part of this section will describe the results of the solubilization of DMPE-B in $C_{12}E_8$ surfactant solutions of varying concentrations and of the effect of solution composition on micelle sizes. This will be followed by discussions of the results of experiments on the interactions between DMPE-B dissolved in the solubilizing surfactant and avidin both well above and below the CMC of $C_{12}E_8$. A theoretical analysis of both the binding of avidin to this ligand above and below the CMC and the light scattering of these aggregates will also be presented.

Solubilization of DMPE-B by $C_{12}E_8$ and Formation of Mixed Micelles. ***Solubility of DMPE-B in Aqueous Surfactant Solutions.*** The methods used for solubilizing DMPE-B in $C_{12}E_8$ solutions are described in the Experimental Section. Using the heating method, a 10 mM $C_{12}E_8$ solution was able to solubilize sufficient phospholipid to produce a solution containing 2.9 mM DMPE-B. However, after several days some precipitate could be observed in the formerly clear solution and thus these solutions were judged to be metastable. Solubility measurements were also made by mixing solid DMPE-B with $C_{12}E_8$ solutions at room temperature. All solutions which solubilized any appreciable DMPE-B contained $C_{12}E_8$ concentrations either at or above the CMC (the CMC for $C_{12}E_8$ is roughly 100 μM; see below). No detectable biotin activity could be observed by titration in the 0.1 mM $C_{12}E_8$ solution. The limit of detection with this method is about 1 μM biotin in the solution to be analyzed. The results indicate that DMPE-B solutions prepared by heating give metastable solutions that only slowly reach equilibrium. However, the equilibrium limit of solubility depends on the $C_{12}E_8$ concentration of the solution and falls between 4–8 mol % of the total solute concentration. More concentrated *metastable* solutions can be prepared and utilized in affinity precipitation for several days by heating the mixture above 70 °C for a few minutes.

Critical Micelle Concentration and Micellar Size. The critical micelle concentrations (CMCs) of aqueous solutions of $C_{12}E_8$ and of $C_{12}E_8$/DMPE-B (7.6:1 mol/mol) mixtures were measured by the surface tension method (Adamson, 1982). The results of this experiment are shown in Figure 2. Also shown in Figure 2 are surface tension values of supernatant solutions following affinity precipitation with avidin which will be discussed below. The pure surfactant $C_{12}E_8$ was determined to have a CMC of approximately 100 μM. This value is in reasonably good agreement with those reported by Rosen et al. (1982) (100 μM) and by Ueno et al. (1981) (85 μM). The addition of DMPE-B to $C_{12}E_8$ in a mole ratio of 1:7.6 had little effect on the CMC; a value of about 100 μM was obtained for these mixtures. The uncertainty in these CMC values is on the order of 10–20 μM.

In order to gauge the number of phospholipid molecules within a $C_{12}E_8$ aggregate, the sizes of both the pure $C_{12}E_8$ surfactant aggregates and those aggregates containing $C_{12}E_8$ and phospholipid were measured by QLS. The results are shown in Figure 3. Since micellar solutions are weakly scattering, we first prepared a concentrated solution of 100 mM $C_{12}E_8$ and measured the apparent micellar diameter. The observed diameter of the $C_{12}E_8$ micelles (56 Å) was in good agreement with the size of 58 Å obtained by Brown et al. (1988) at 25 °C. Nilsson et al. (1983) report a value of 62 Å for the diameter of $C_{12}E_8$ micelles. The $C_{12}E_8$ micelle size was observed to be independent of $C_{12}E_8$ concentration from 100 mM to less than 1 mM. Using the group volumes for methyl, methylene, and ethylene oxide groups suggested by Tanford (1980), one can calculate an approximate molecular volume for the $C_{12}E_8$ molecule of 885 $Å^3$. Assuming that the micelle contains no solvent, an aggregation number of 104 is obtained for a micelle diameter of 56 Å. This is in reasonable agreement with an aggregation number of 127 obtained for $C_{12}E_8$ micelles by Brown et al. (1988) based on micelle molecular weights determined by static light scattering. Solutions less concentrated than about 1 mM were so weakly scattering that it was not possible to obtain an autocorrelation function from which to calculate an effective diameter.

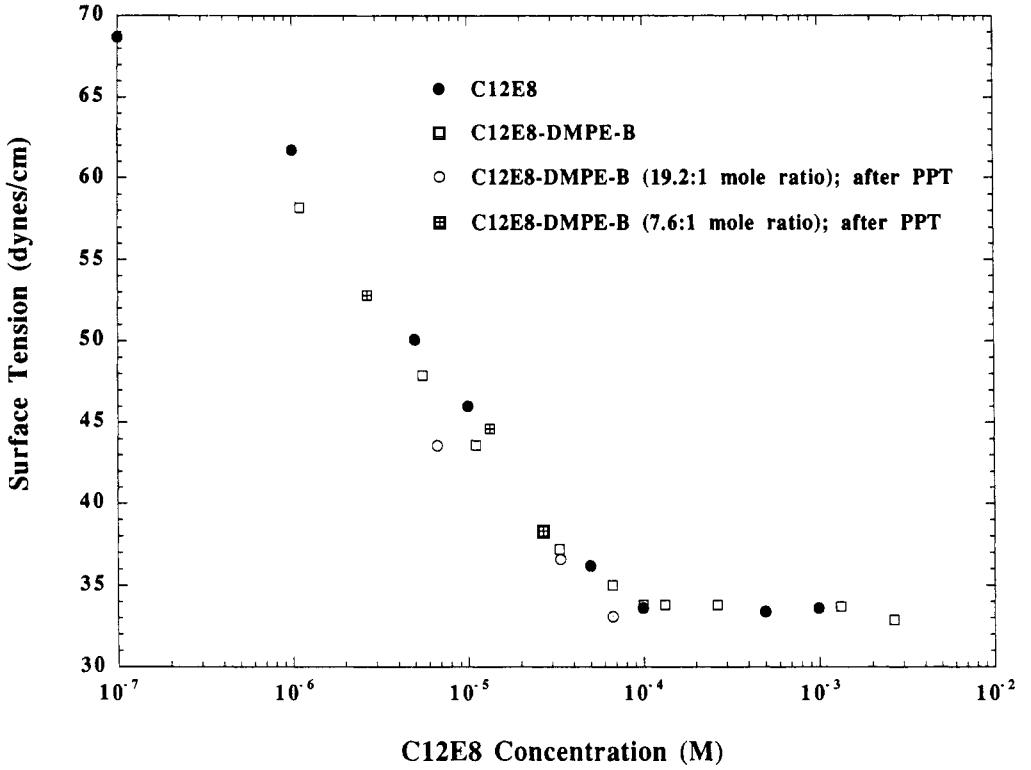

Figure 2. Surface tension measurements of $C_{12}E_8$ and $C_{12}E_8$/DMPE-B solutions. Surface tensions of aqueous solutions of $C_{12}E_8$ and $C_{12}E_8$/DMPE-B (7.6:1 mol/mol) mixtures in standard buffer. The approximate breakpoint in the surface tension curves corresponds to the CMC of the surfactant solution. In addition, (×) and (+) correspond to surface tensions of DMPE-B/$C_{12}E_8$ mixtures—7.6:1 and 19.6:1 mol/mol, respectively—after precipitation with avidin and filtration of the supernatant through a 0.2-μm filter.

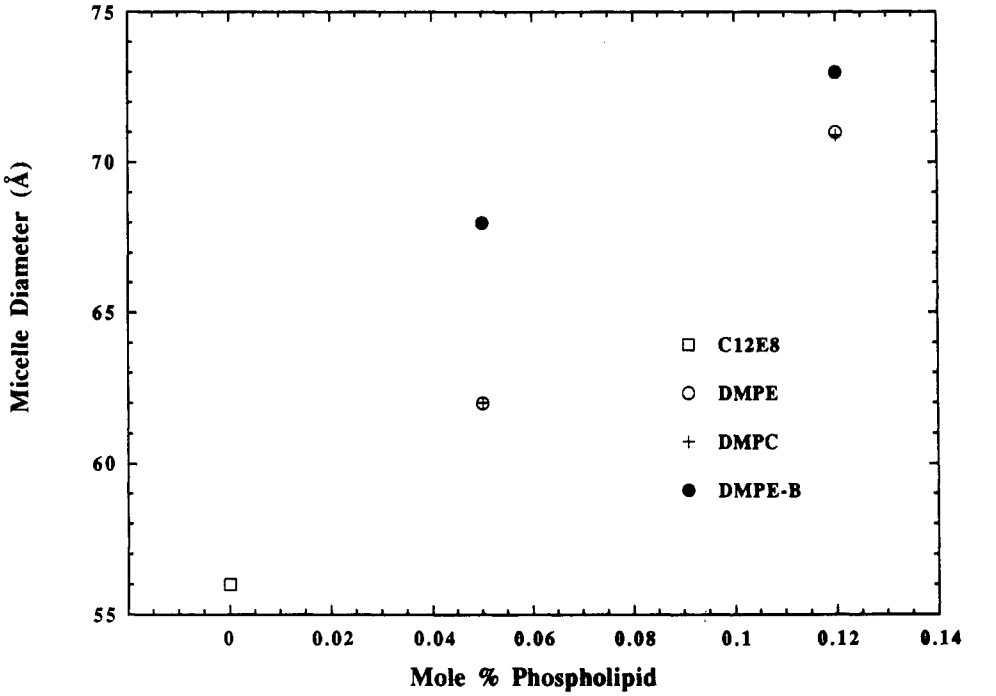

Figure 3. Micelle size and phospholipid concentration. Points represent intensity-weighted mean diameters of mixed $C_{12}E_8$/phospholipid micelles determined in standard buffer at 25 °C. Phospholipids studied were DMPE, DMPC, and DMPE-B. Micelle sizes at a specific phospholipid mol % were determined to be independent of total surfactant concentration in the range from 1 mM to 100 mM.

Micellar solutions were next prepared containing solubilized DMPC and DMPE in $C_{12}E_8$ at 5 and 12 mol % phospholipid. This was achieved by heating the mixtures to result in metastable micellar solutions as described above. The $C_{12}E_8$ concentration was varied from 1 to 100 mM. Insertion of these phospholipids into the surfactant micelle caused an increase in diameter proportional to the mol % of phospholipid in the micelle (Figure 3). For example, a 5 mol % DMPE or DMPC (20:1 mole ratio) concentration in the micelles increases the diameter from 56 Å for the phospholipid-free micelle to 62 Å for the phospholipid-containing micelle. The micelle size at 5 mol % phospholipid was independent of $C_{12}E_8$ concentration within ±1 Å. Using Tanford's method for calculating molecular volumes, the molecular volumes of DMPE, DMPC, and DMPE-B were calculated to be 1060, 1060,

Table I. Mixed $C_{12}E_8$/Phospholipid Micelle Sizes, Aggregation Numbers, and Phospholipids per Micelle

	DMPE	DMPC	DMPE-biotin	
mole % phospholipid	5	12	5	12
micelle size[a] (Å)	62	71	68	73
aggregation number[b]	139	207	182	218
no. of phospholipid molecules per micelle	7	25	9	26

[a] Micelle size obtained from QLS. [b] Aggregation number obtained from $N_{agg} = \pi d^3/6M_s$, $\bar{M}_s = X_{C_{12}E_8}M_{C_{12}E_8} + X_{Phos}M_{Phos}$.

and 1298 Å^3, respectively. Assuming the mixed $C_{12}E_8$–phospholipid micelles are spherical, it is possible to compute micelle aggregation numbers and the average number of phospholipid molecules per micelle for each of the micelle sizes measured and shown in Figure 3. These calculations are summarized in Table I. Two trends are clear from the data presented in Figure 3 and the computed aggregation numbers presented in Table I: (1) the micelle size increases with increased phospholipid concentration for each of the phospholipids studied and (2) with increasing phospholipid size (DMPE, DMPC < DMPE-B), the micelle size is larger at the same phospholipid content with the larger phospholipid.

Binding of Avidin to DMPE-B/$C_{12}E_8$ Micelles Well Above the CMC. ***Experimental Results.*** The kinetics of binding of DMPE-B in micelles of $C_{12}E_8$ to avidin was studied at three different molar ratios of DMPE-B to avidin (5.5, 11.1, and 32.2). In these experiments, the concentration of avidin was kept constant at 1 μM and the concentration of $C_{12}E_8$ was chosen to be 1 mM, far in excess of its CMC of 100 μM. Even at the highest molar ratio of DMPE-B to avidin (32.2), the molar ratio of DMPE-B to $C_{12}E_8$ is only 3.2%. One can conclude that less than 6 molecules of DMPE-B per micelle are present in these experiments. The association of avidin with DMPE-B in these micelles was monitored by measuring the hyperchroic shift in the UV spectrum of avidin (231.5 nm) upon binding to the biotinyl group. The magnitude of the hyperchroic shift measured when a 1 μM solution of avidin is completely bound with biotin is on the order of 0.1 absorbance units. Figure 4 shows the results obtained for the association of avidin with DMPE-B solubilized in $C_{12}E_8$ well above the CMC. The magnitude of the hyperchroic shift observed in this case is very similar to what is measured between avidin and biotin alone. It is clear that as the ratio of DMPE-B to avidin increases, the kinetics of binding increase.

The low values of absorbance under these conditions suggest that there is little or no precipitation or aggregation of protein when the solubilizing surfactant concentration is sufficiently high. The avidin is able to bind to the DMPE-B that is solubilized in the micelles, as evidenced by the clearly measured hyperchroic shift, but the high concentration of $C_{12}E_8$ prevents the formation of any aggregates. As will be seen in a subsequent section, when the avidin is allowed to bind to DMPE-B that is solubilized using $C_{12}E_8$ concentrations below the CMC when there are no micelles present, the absorbance values rise as high as 1.0, and protein aggregation or precipitation is clearly evident.

Theoretical Analysis. If the interpretation of the above experimental observations of the kinetics and equilibrium of binding is correct, it should be possible to analyze these data by considering the avidin molecule as having four equivalent and independent binding sites, each of which can associate with DMPE-B which is solubilized in the micelles in solution. The association of DMPE-B to four binding sites on a single avidin molecule can be represented by the stoichiometric formula

$$AB_i + B \underset{k'}{\overset{k}{\rightleftharpoons}} AB_{i+1}, \quad i = 0, 1, 2, 3 \tag{1}$$

where AB_i denotes an avidin molecule with i DMPE-B molecules bound to it. In the above set of reactions, the forward rate constant k and the reverse rate constant k' are assumed to be the same for each of the four reactions; i.e., each binding step can be assumed to be identical and independent. The time rate of change of each of the types of bound avidin molecules is therefore

$$\frac{d\hat{C}_{AB}}{dt} = k\hat{C}_A\hat{C}_B - k'\hat{C}_{AB} - k\hat{C}_{AB}\hat{C}_B + k'\hat{C}_{AB_2} \tag{2}$$

$$\frac{d\hat{C}_{AB_2}}{dt} = k\hat{C}_{AB}\hat{C}_B - k'\hat{C}_{AB_2} - k\hat{C}_{AB_2}\hat{C}_B + k'\hat{C}_{AB_3} \tag{3}$$

$$\frac{d\hat{C}_{AB_3}}{dt} = k\hat{C}_{AB_2}\hat{C}_B - k'\hat{C}_{AB_3} - k\hat{C}_{AB_3}\hat{C}_B + k'\hat{C}_{AB_4} \tag{4}$$

$$\frac{d\hat{C}_{AB_4}}{dt} = k\hat{C}_{AB_3}\hat{C}_B - k'\hat{C}_{AB_4} \tag{5}$$

In eqs 2–5, the overbar denotes the concentration of AB_i in which the specific sites bound on the avidin molecule are distinguishable. For example, an avidin molecule with one bound DMPE-B molecule can occur in one of four distinguishable ways. Thus, there is an equivalent rate equation for each type of AB_1 species. In order to obtain the total concentration of bound species, the above concentrations must be weighted by the number of ways in which such a distinguishable bound species can be formed. The resulting expression for total concentration of bound species AB_n is (van Holde 1971)

$$C_{AB_n} = \frac{4!}{(4-n)!n!}\hat{C}_{AB_n} \tag{6}$$

The concentration of total unbound or free avidin is therefore

$$C_A = C_A^\circ - \sum_{n=1}^{4}\frac{4!}{(4-n)!n!}\hat{C}_{AB_n} \tag{7}$$

and the concentration of unbound or free DMPE-B is

$$C_B = C_B^\circ - \sum_{n=1}^{4}\frac{4!}{(4-n)!n!}(n\hat{C}_{AB_n}) \tag{8}$$

Equations 5–8 were made dimensionless by defining free and bound avidin concentrations and free DMPE-B concentrations according to

$$y_{AB_i} = \frac{C_{AB_i}}{C_A^\circ}, \quad y_A = \frac{C_A}{C_A^\circ}, \quad y_B = \frac{C_B}{C_A^\circ} \tag{9}$$

where C_A° is the initial avidin concentration. The time was made dimensionless according to

$$\xi = kC_A^\circ t \tag{10}$$

Equations 2–5 can be used to analyze the data in Figure 4 to obtain values of the equilibrium binding constant $K_{eq} = k/k'$ and the forward rate constant k. For proteins with multiple binding sites which are identical and independent,

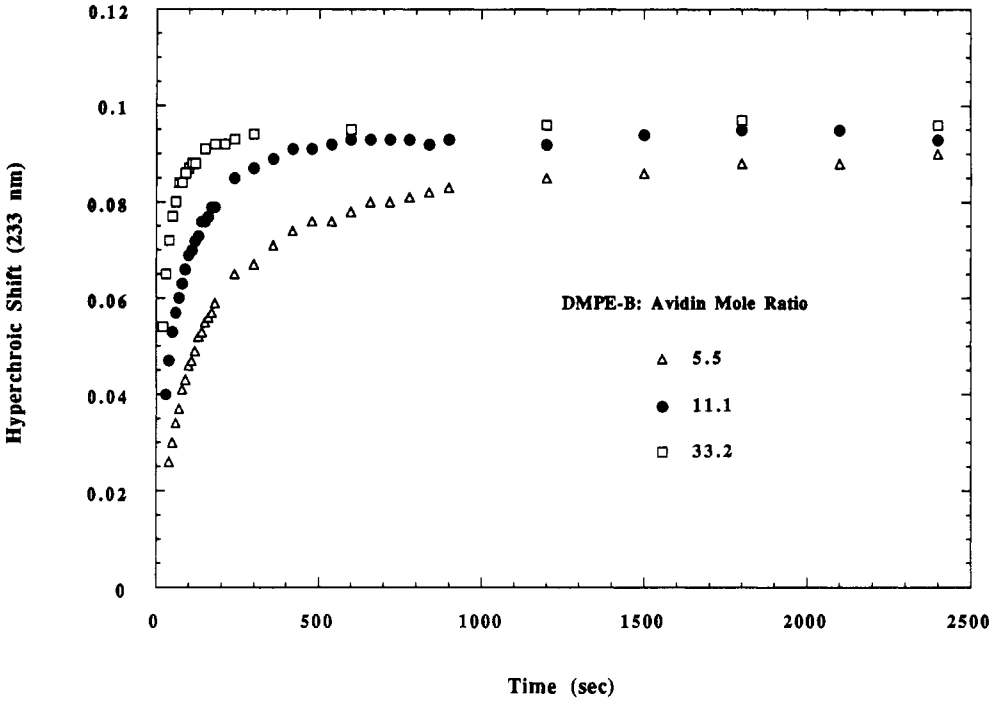

Figure 4. Time course for micellar-DMPE-B binding to avidin. Avidin (100 μL; 30 μM) and 0.1 M $C_{12}E_8$, sufficient to give a final concentration of 1 μM avidin and 1 mM $C_{12}E_8$, were combined with standard buffer in the sample and reference cuvette of a spectrophotometer and the absorbance was zeroed. At time t = 0, an appropriate volume of DMPE-B solution (10–60 μL; 1.66 mM in standard buffer containing 50 mM $C_{12}E_8$) was added to the sample cuvette. The final volume in the cuvette was 3.0 mL. The absorbance change at 231.5 nm was monitored until no further increase was observed.

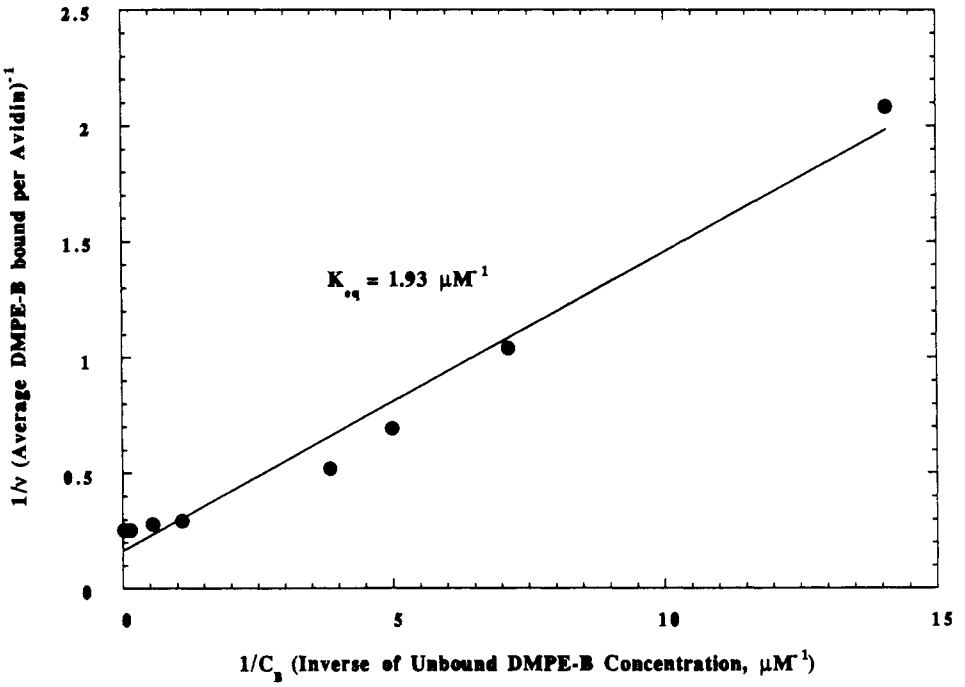

Figure 5. Scatchard plot for determination of micellar-DMPE-B avidin binding constant. See Experimental Section for a description of the procedure.

the equilibrium constant can be determined from a Scatchard plot (van Holde 1971):

$$\frac{1}{\nu} = \frac{1}{n} + \frac{1}{nK_{eq}C_B} \tag{11}$$

where ν denotes the number of bound ligand molecules per protein and n is the total number of binding sites per protein. Equation 11 can be derived by setting the time derivatives in eqs 2–5 equal to zero and combining the right-hand side of each expression with eqs 7 and 8. By measuring the equilibrium hyperchroic shift S of 1 μM avidin solutions to which increasing amounts of DMPE-B in 1 mM $C_{12}E_8$ micelles had been added, the quantity ν was calculated as

$$\nu = \frac{4S}{S_{max}} \tag{12}$$

In eq 12, S_{max} is the maximum hyperchroic shift possible for a 1 μM solution corresponding to complete binding of all of the active sites on the avidin molecule. This value was determined to be 0.1 absorbance units for a 1 μM avidin solution. The resulting Scatchard plot is shown in

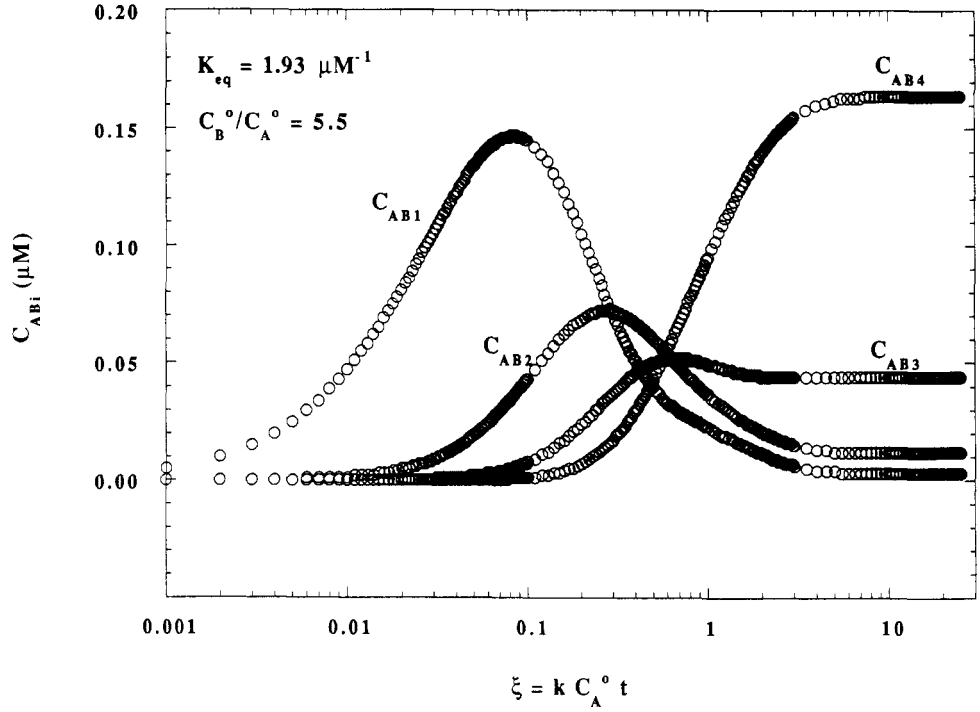

Figure 6. Predicted concentrations of micellar-DMPE-B species as a function of dimensionless time. The values of C_{AB_i} were calculated by solving eqs 5–8 using Gear's method, an equilibrium binding constant of 1.93 μM^{-1}, and a molar ratio of initial ligand concentration to initial avidin concentration of 5.5.

Figure 5, and from it a value of 1.93 μM^{-1} is determined for K_{eq}. The equilibrium binding data reported in Figure 5 resulted from experiments performed independently from those which generated the kinetic data shown in Figure 4. It should be noted that the binding constant of DMPE-B in $C_{12}E_8$ micelles to avidin reported here is much lower than the reported binding constant (Green, 1963) of biotin to avidin ($\approx 10^{15}$ M^{-1}). Part of this difference may be due to the diminished access of the biotin group for the avidin binding pocket when biotin is immobilized on $C_{12}E_8$ micelles of 60–70-Å diameter. It is known that the avidin binding sites are recessed approximately 7–9 Å from the surface of the protein. Since the ethoxy polar head groups are likely to be much more extended or exposed in the aqueous phase than the smaller biotin moiety, a significant reduction in binding accessibility can be expected. The binding constant of DMPE-B in micelles for avidin is of the same order of magnitude as other affinity interactions, such as enzyme–inhibitor and antigen–polyclonal antibody interactions.

The time dependence of the binding of DMPE-B in $C_{12}E_8$ micelles to avidin was computed for varying values of C_B°/C_A° by solving eqs 2–5 subject to the appropriate initial conditions using Gear's method (Gear, 1971; IMSL Math Library, 1987). A typical result for the concentrations of AB_i as a function of dimensionless time ξ for the case of C_B°/C_A° = 5.5 is shown in Figure 6. The time dependence of each of the bound protein concentrations is as expected; proteins with singly bound ligand are formed rapidly, achieve a maximum concentration, and then are depleted as additional ligands bind. At this ratio of DMPE-B to avidin, the predominant species at long time is fully-bound avidin AB_4. The total concentration of bound ligand is simply the difference between C_B° and C_B obtained by rearranging eq 8.

$$\text{bound ligand} = C_B^\circ - C_B = \sum_{n=1}^{4} \frac{4!}{(4-n)!n!} n C_{AB_n} \quad (13)$$

The value of the forward rate constant for binding can be determined by comparison of the prediction of bound ligand concentration with that measured experimentally. The measured bound ligand concentration is simply

$$\text{bound ligand}_{exp} = C_A^\circ \nu = \frac{C_A^\circ 4S}{S_{max}} \quad (14)$$

The value of k can be chosen to obtain the best agreement between the predicted and experimental bound ligand concentrations and is used to nondimensionalize the experimental time scale according to eq 10. The value of k obtained is independent of the ratio C_B°/C_A° and equal to 2000 M^{-1} s^{-1}. The agreement between the model and the experimental data is illustrated in Figure 7 for the three ratios C_B°/C_A° used experimentally and is reasonably good over the range of dimensionless time.

Binding of Avidin to DMPE-B in Submicellar Aggregates: Affinity Precipitation. The experiments performed above the CMC of $C_{12}E_8$ indicate that no precipitation of avidin occurs in the presence of $C_{12}E_8$ micelles. We now describe experiments performed *below* the CMC of $C_{12}E_8$ for which the DMPE-B is solvated by surfactant molecules in submicellar aggregates. It is at these concentrations of $C_{12}E_8$ that affinity precipitation is observed to occur.

Experimental Results. *Effect of DMPE-B-to-Avidin Mole Ratio on Precipitation.* Avidin at a 1 μM concentration was allowed to bind to DMPE-B present in a concentration range of 1–18.75 μM and a constant concentration of $C_{12}E_8$ of 75 μM. These experiments were performed by adding to the avidin solution different aliquots of solubilized DMPE-B/$C_{12}E_8$ mixtures whose concentrations were adjusted so that the desired final concentrations in the sample cuvette were obtained. Over time, the solutions became turbid, so that it was possible to monitor the course of precipitation by measuring the ultraviolet absorbance due to scattering at 233 nm. The results are shown in Figure 8. It should be noted that all of the recorded absorbance values shown in Figure 8 were obtained when the $C_{12}E_8$ concentration is just *below* the

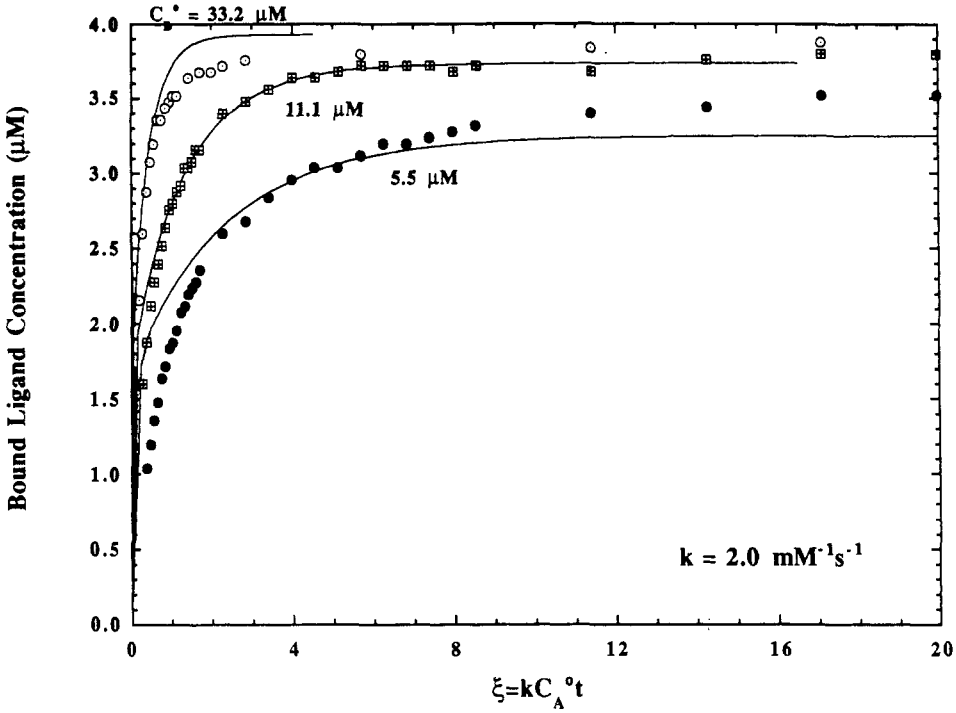

Figure 7. Comparison of observed and calculated time course for kinetics of micellar-DMPE-B and avidin binding. Theoretical bound ligand concentrations were obtained by solving for C_{AB_n}, according to eqs 5–8, and summing according to eq 16. Experimental bound ligand concentrations were obtained from the raw data of Figure 6 according to eq 17.

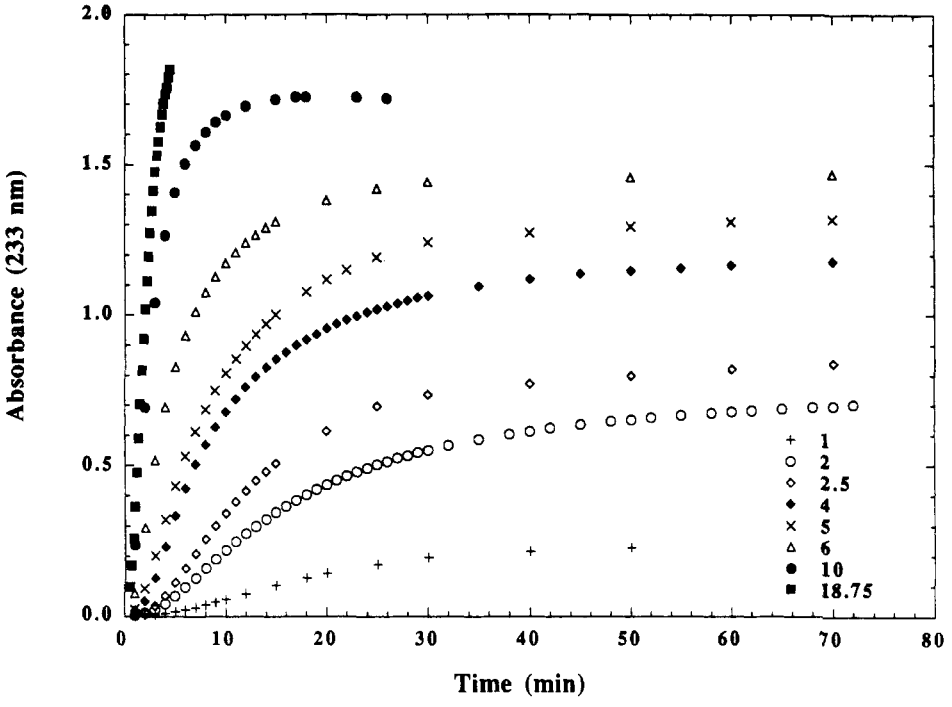

Figure 8. Effect of DMPE-B: avidin mole ratio on affinity precipitation. Sufficient 0.30 mM DMPE-B containing 1 mM $C_{12}E_8$ and 0.01 M $C_{12}E_8$, both in standard buffer, were added to an avidin solution to give final concentrations of 1 μM avidin, 75 μM $C_{12}E_8$, and DMPE-B concentrations varying from 1 to 18.75 μM. The absorbance at 233 nm was monitored until no further change in absorbance was detected.

CMC of $C_{12}E_8$. Under these conditions, it is not possible to detect the presence of any micelles through quasielastic light scattering, and the DMPE-B exists in metastable submicellar aggregates which may contain only a few molecules of $C_{12}E_8$. Prior to the addition of DMPE-B to the avidin solution, the DMPE-B was solubilized in $C_{12}E_8$ at concentrations above the CMC and the $C_{12}E_8$ concentration falls below the CMC only upon addition of the concentrated solution to the sample vial containing protein.

It is clear from Figure 8 that the rate of rise of the measured absorbance increases significantly with increasing ratios of DMPE-B to avidin at a fixed $C_{12}E_8$ concentration. It is also evident that the final value of the turbidity at long times increases as well with increasing ratios of DMPE-B to avidin. If the results of Figure 8, obtained below the CMC of $C_{12}E_8$, are compared to the results of Figure 4, obtained well above the CMC of the surfactant, it is clear that the absorbance values obtained

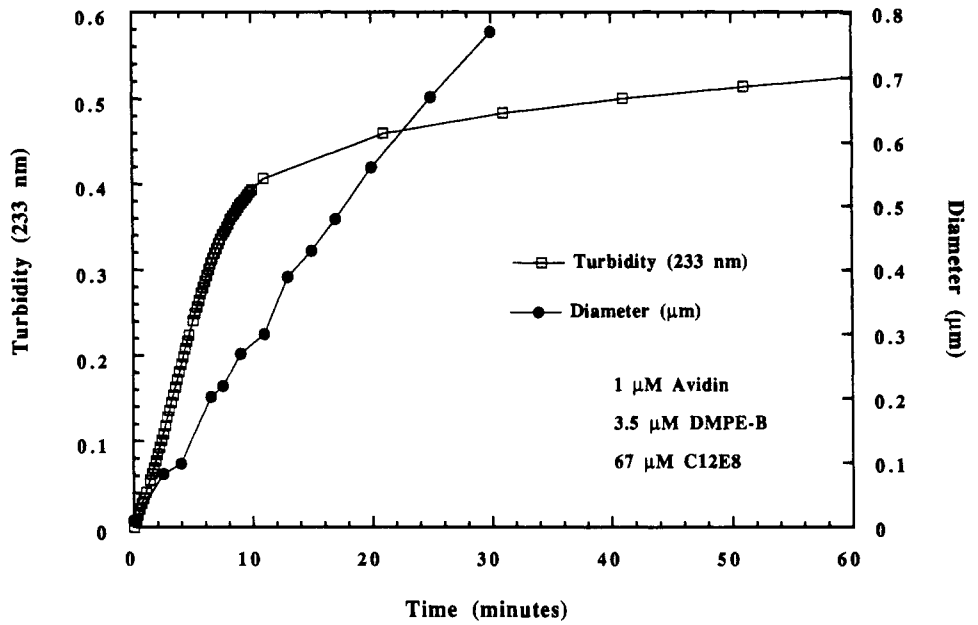

Figure 9. Size growth of avidin–DMPE-B (DMPE–XX-B) aggregates as determined by turbidity and QLS. DMPE-B (53 μM) in standard buffer containing 1 mM $C_{12}E_8$ was added to a QLS cuvette that contained a solution of avidin in standard buffer. Final concentrations were 3.5 μM DMPE-B, 1 μM avidin, and 67 μM $C_{12}E_8$ in 3.0 mL. Particle size measurements were made at intervals as the aggregation proceeded. Closed circles denote mean particle sizes as measured by QLS; open squares denote absorbance values obtained from an identical aggregation mixture monitored at 233 nm as a function of time in spectrophotometer cuvette.

in the absence of micelles greatly exceed the maximum absorbance values determined from the hyperchroic shift due to biotin to avidin binding in the presence of micelles. This increase in absorbance is the direct result of the formation of protein aggregates below the CMC of $C_{12}E_8$. The growth of these aggregates can be followed by QLS, and they can be separated from the solution by centrifugation. As shown by Guzman et al. (1990), these precipitates contain highly pure avidin, even when the precipitation is allowed to occur in partially purified egg white solutions. Guzman et al. (1990) also showed that the precipitation occurs only in the presence of biotin-modified phospholipid. Control experiments in which avidin is exposed to DMPE/$C_{12}E_8$ solutions which do not contain biotin coupled to the phospholipid do not exhibit precipitation. These results, together with those of Figure 4 above the CMC, offer conclusive evidence that the aggregates that are formed when the $C_{12}E_8$ concentration is below the CMC are the result of binding of avidin to DMPE-B, followed by precipitation of ligand-bound protein due to the absence of micelles that can keep these aggregates solubilized. In effect, what is accomplished is a temporary modification of the solubility of the protein due to the attachment of the relatively large and hydrophobic phospholipid molecule. In the presence of DMPE-B/$C_{12}E_8$ micelles, the surfactant can solubilize these ligand-bound proteins and the absorbance never exceeds the hyperchroic shift values. In the absence of micelles, the absorbance values increase due to the presence of the relatively large aggregates.

Size Growth of Avidin Aggregates Measured by Quasielastic Light Scattering (QLS). The turbidity, monitored at 233 nm, is a function of the number and size of the aggregates that form. In addition to monitoring affinity precipitation by measurement of turbidity, the size of the affinity precipitates were measured as a function of time by QLS. This was accomplished by adding a solution of DMPE-B in $C_{12}E_8$ to an avidin solution such that the final concentrations were 1 μM avidin, 3.6 μM DMPE-B, and nominally 70 μM $C_{12}E_8$. The turbidity of the precipitating solution was then monitored at 233 nm, and direct size measurements were made at intervals on an identical solution placed in the QLS compartment. The results of this experiment with DMPE-B are shown in Figure 9. As turbidity increased from 0 to 0.5 absorbance units over the first 30 min of precipitation, the mean aggregate size increased from a few hundred angstroms to about 0.8 μm. Measurements of aggregate size beyond 1 μm size were not made because multiple scattering occurs in this size range and this complicates the interpretation of the autocorrelation function. It should be noted that these particle sizes are only approximate and are weighted strongly by the larger particles in the distribution. Nonetheless, the results suggest that for a given set of precipitation conditions, a relationship exists between turbidity and mean particle size, both of which can be used as a measure of the time course of the aggregation.

Fate of $C_{12}E_8$ in Precipitation. In order to determine the fate of the nonionic surfactant $C_{12}E_8$ in the precipitation mechanism, experiments were performed in which avidin was precipitated by DMPE-B/$C_{12}E_8$ solutions at concentrations near the CMC and the surface tension of the residual supernatant solution was measured, after separating the affinity precipitate, to determine the $C_{12}E_8$ concentration after precipitation. These results are reported in Figure 2, along with the surface tension measurements performed on pure $C_{12}E_8$ and $C_{12}E_8$/DMPE-B (12 mol %) solutions. In addition, two dilutions of these supernatants with buffer were made and the surface tensions of these solutions were measured. The results are plotted in Figure 2 as a function of the *initial* $C_{12}E_8$ concentration and the value that would be obtained upon dilution if all of the $C_{12}E_8$ remained in solution after precipitation. As can be seen from the results in Figure 2, these surface tension values fall close to those values measured for pure $C_{12}E_8$ and for $C_{12}E_8$/DMPE-B solutions. This suggests that very little of the nonionic surfactant $C_{12}E_8$ actually precipitates with the avidin–phospholipid complexes.

Precipitation of Avidin by DMPE-B at $C_{12}E_8$ Concentrations *Near* the CMC. The experiments on binding of DMPE-B to avidin described thus far were performed

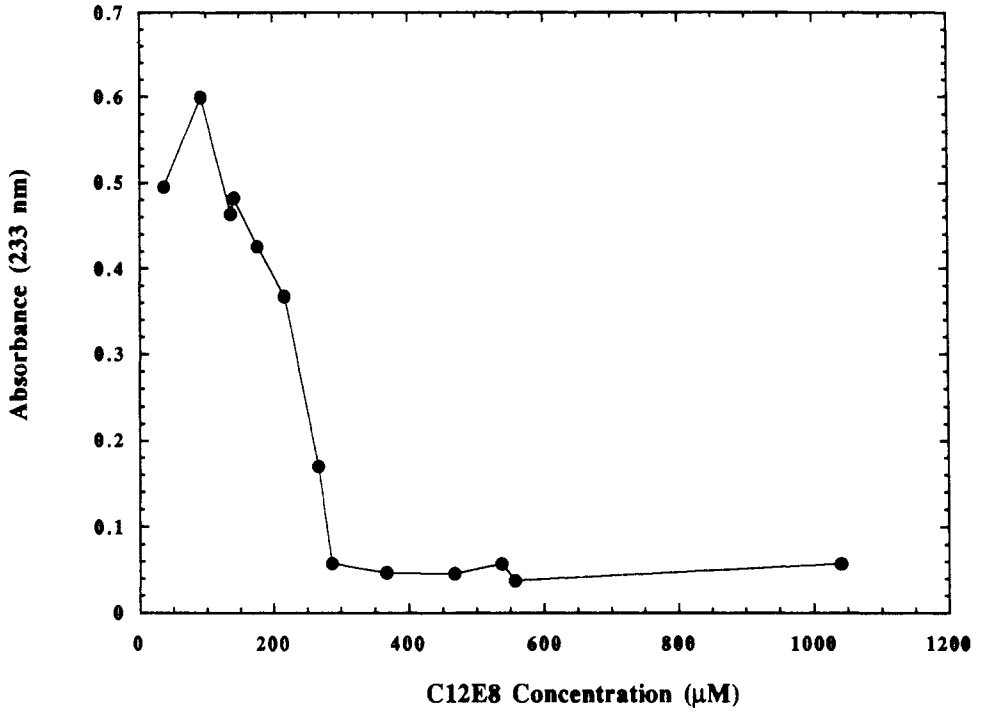

Figure 10. Effect of $C_{12}E_8$ concentration on affinity precipitation as gauged by maximum absorbance. Avidin (30 μM), $C_{12}E_8$ (52 mM), and buffer were combined in a spectrophotometer curvette. At time t = 0, sufficient DMPE-B (0.12 mM) containing $C_{12}E_8$ was added to the cuvette in order to give final concentrations of 1 μM avidin, 4 μM DMPE-B, and 50–1050 μM $C_{12}E_8$ in a total volume of 3.0 mL. Absorbance was monitored at 233 nm until no further increase was observed. The values reported are maximum absorbances.

at $C_{12}E_8$ concentrations either *far above* the CMC (>1 mM), at which avidin is observed to *not* precipitate, or *just below* the CMC (<0.1 mM) in which precipitation occurs. Experiments are now described in which the effect of *intermediate* $C_{12}E_8$ concentrations *near* the CMC on affinity precipitation is explored.

Experiments were performed in which the phospholipid-to-protein ratio was maintained constant at 4:1 and the $C_{12}E_8$ concentration was varied from about 50 μM to approximately 1 mM. This corresponds to a concentration range from just below the CMC to about a factor of 10 greater than the CMC. The results of these experiments are shown in Figure 10. Precipitation is observed, indicated by maximum turbidity values far exceeding that of the hyperchroic shift alone, at $C_{12}E_8$ concentrations up to about 290 μM. Since the CMC for DMPE-B/$C_{12}E_8$ is about 100 μM, then affinity precipitation *can* occur, although not very efficiently, when the majority of the phospholipid is solubilized in micelles, as well as when the phospholipid is solubilized in small aggregates.

The observation of a limiting $C_{12}E_8$ concentration above which precipitation does not occur suggests that dilution of the ligand-modified phospholipid among the micellar aggregates prevents precipitation. Thus, at 290 μM $C_{12}E_8$, DMPE-B is present at 1.2 mol % (85:1 $C_{12}E_8$/DMPE-B), and from QLS measurements at this concentration we can estimate an approximate aggregation number of 123 for the DMPE-B/$C_{12}E_8$ mixed micelles. Combining these two values gives a ligand/micelle ratio of about 1.5:1. Precipitation does *not* occur at this DMPE-B concentration indicating that less than two ligand-modified phospholipid molecules per micelle will not support aggregation.

Theoretical Analysis. *Modeling of Precipitation of DMPE-B-Bound Avidin.* In order to obtain theoretically based estimates of the rate constants characterizing precipitation, of the yields of precipitation, and of the size of the precipitates as measured in either a turbidimetric or light-scattering experiment, the precipitation of avidin molecules to which DMPE-B has bound was modeled as a sequence of stepwise agglomeration reactions using von Smoluchowski kinetics (Drake, 1972):

$$\begin{aligned} A^* + A^* &\rightleftharpoons (A^*)_2 \\ (A^*)_2 + A^* &\rightleftharpoons (A^*)_3 \\ (A^*)_i + A^* &\rightleftharpoons (A^*)_{i+1} \end{aligned} \tag{15}$$

In the above sequence of reactions, A* represents an avidin molecule to which at least one DMPE-B molecule has bound. Since the ligand-binding step is relatively fast (Figure 4) as compared to precipitation (Figure 8), the initial concentration of A* can be calculated by dividing the equilibrium bound ligand concentration by the number of sites on avidin. This quantity will be termed N_o and represents the concentration of precipitable protein molecules, i.e., the seed particle concentration.

$$N_o = \frac{\nu}{4} C_A^{\,o} = \frac{K_{eq} C_B}{1 + K_{eq} C_B} C_A^{\,o} \tag{16}$$

Assuming irreversible aggregation, the time rate of change of an aggregate of i protein molecules is given by

$$\frac{dC_{(A^*)_i}}{dt} = a_{1,i-1} C_{(A^*)} C_{(A^*)_{i-1}} - a_{1,i} C_{(A^*)} C_{(A^*)_i} \tag{17}$$

where $a_{1,i}$ denotes the rate constant corresponding to a monomer and an i-mer aggregating to form an i+1-mer. The functional forms of a_{nm} for which analytical solutions of eq 17 are known are quite limited. Drake (1972) has reviewed the literature, primarily from the aerosol field, in which eq 17 and its variants have been solved. One important case which yields aggregate size distributions which seem to agree well with latex–antibody agglutination aggregate distributions (von Schulthess et al., 1980) is that given by

$$a_{nm} = \beta(n + m) \tag{18}$$

where β is a constant independent of aggregate size. Using

the form of the individual rate constants given by eq 18, the infinite set of rate equations represented by eq 17 for $i = 2$ to ∞ can be solved analytically by Laplace transform techniques (Drake, 1972) to yield the following expression for the concentration of n-mer:

$$C_{(A^*)_n} = \frac{N_0(1-b)e^{-nb}(nb)^{n-1}}{n!} \tag{19}$$

In the above expression, b represents a rescaled time variable which gauges the extent of precipitation and is given by

$$b = 1 - \frac{N}{N_0} = 1 - \exp(-\beta N_0 t) \tag{20}$$

In eq 20, N is the total molar concentration of protein aggregates at any instant in time:

$$N = \sum_{n=1}^{\infty} C_{(A^*)_n} \tag{21}$$

while N_0 represents the total concentration of protein *monomer* in aggregates

$$N_0 = \sum_{n=1}^{\infty} nC_{(A^*)_n} \tag{22}$$

Since N_0/N is the average number of proteins in the aggregates, the quantity b is seen to be a measure of the extent of aggregation. Initially, all of the protein is present as monomers and b is zero. At long times, N decreases as the average aggregate size increases and b approaches unity. At infinitely long times, the Smoluchowski theory with the rate constants given by eq 18 predicts an approach to one large aggregate. In reality, the protein aggregates achieve a limiting size due to collisions that break up aggregates at a rate equal to that at which they are being formed. In order to account for this, we follow the approach of von Schulthess et al. (1980) and truncate b at a limiting value b_∞. The time dependence of b is then given by

$$b = b_\infty(1 - \exp(-\beta N_0 t)) \tag{23}$$

Equations 19 and 23 provide for an analytical description of the time dependence of aggregate size distribution. The results depend on three parameters: β, the rate constant appearing in eq 18, b_∞, and N_0, the initial molar concentration of seed protein molecules. Given the aggregate size distribution, it is possible to compute the turbidity of the aggregating suspension.

Modeling of Turbidity of Precipitating Protein Mixture: Mie Theory. The turbidity due to scattering of a monodisperse collection of particles of radius a_n is given by (van de Hulst, 1957)

$$\tau_n = N_A C_{(A^*)_n} \pi a_n^2 Q_{ext} \tag{24}$$

where $C_{(A^*)_n}$ is the molar concentration of scatterers comprised of n protein molecules, Q_{ext} is the extinction coefficient in units of absorbance per unit path length corresponding to the particles, and N_A is Avogadro's number. Van de Hulst (1957) presents an expression for Q_{ext} for Mie scattering (particles with diameters of the order of the wavelength of the incident light) which is accurate for values of the ratio of refractive indices of solvent and scatterer which are close to unity:

$$Q_{ext} = 2 - \frac{4}{\rho}\sin\rho + \frac{4}{\rho^2}(1 - \cos\rho) \tag{25}$$

Table II. Experimental Variables Set by Details of Scattering Experiment

variable	symbol	value
refractive index of 0.2 M ammonium carbonate buffer[a]	m_2	1.337
refractive index of protein aggregate[b]	m_1	$1.337\epsilon + 1.50(1-\epsilon)$
void fraction of protein aggregate[c]	ϵ	0.6
wavelength of incident light in a vacuum	λ_{vac}	2330 Å
radius of avidin molecule[d]	a_1	35 Å

[a] Reference: *CRC Handbook of Chemistry and Physics*, 56th ed.; CRC Press: Boca Raton, FL, 1975. [b] Refractive index of protein was taken to be 1.50, consistent with that reported for other globular proteins. [c] The void fraction was varied from 0.6 to 0.95, which is in the range 0.3–0.9 of that reported for protein crystals (McPherson, 1991). [d] This value was obtained by quasielastic light scattering of dilute avidin solutions.

The quantity ρ denotes the scattering vector given by

$$\rho = \frac{4\pi a_n m_2}{\lambda_{vac}}\left|\frac{m_1}{m_2} - 1\right| \tag{26}$$

In the definition of ρ, a_n denotes the radius of a protein aggregate containing n protein molecules, m_1 and m_2 are the refractive indices of the protein aggregate and solvent, respectively, and λ_{vac} is the wavelength of the incident light which is being scattered. Equation 25 is expected to be valid for turbidimetric scattering by protein precipitates because the refractive index of the protein precipitates, which include a large amount of water, should be close to that of the aqueous background. For a polydisperse collection of scatterers, the turbidity due to scattering from particles of each size must be integrated to obtain the total turbidity

$$\tau = N_A\int_1^\infty C_{(A^*)_n}\pi a_n^2 Q_{ext}(a_n)\,dn \tag{27}$$

The dependence of the n-mer protein aggregate radius on the radius of an individual protein molecule can be obtained by assuming the protein aggregates are roughly globular or spherical and that the volume fraction of solvent contained in the aggregate is ϵ:

$$a_n = a_1 n^{1/3}(1-\epsilon)^{-1/3} \tag{28}$$

Combination of eqs 19, 27, and 28 and the use of Stirling's approximation for large n (von Schulthess et al., 1980) yields the following expression for the turbidity of the aggregating suspension of protein normalized with respect to N_0:

$$\frac{\tau}{N_A N_0} = \left(\frac{\pi}{2}\right)^{1/2} a_1^2(1-\epsilon)^{-2/3}\frac{1-b}{b}\int_1^\infty Q_{ext}e^{-\mu n}n^{-5/6}\,dn \tag{29}$$

where

$$\mu = -\ln b + b - 1 \tag{30}$$

The quantities in eq 29 which depend explicitly on the particular details of the turbidimetric experiment are listed in Table II. In the calculations of turbidity according to equation 29, the value of ϵ, the volume fraction of solvent in the protein precipitate, was varied from 0.6 to 0.95 to determine its effect on the predicted turbidity and, as shown below, the dependence of diameter as measured by quasielastic light scattering on time. These values of ϵ are in the range of solvent volume fractions (0.3–0.9) reported by McPherson (1991) for protein crystals. One might expect protein precipitates obtained in the fashion described in this paper to contain more entrained solvent than protein *crystals* grown from a supersaturated solution.

Table III. Values of Solvent Volume Fraction ϵ and Corresponding Long-Time b Value Used in Smoluchowski–Mie Theory Calculations of Turbidity

ϵ	b_∞	$t_{1/2}$*	ϵ	b_∞	$t_{1/2}$*
0.6	0.98786	3.776	0.85	0.99546	4.774
0.7	0.99090	4.075	0.90	0.99697	5.184
0.8	0.99395	4.483	0.95	0.99847	5.884

In order to compare the prediction of eq 29 with the experimental data presented in Figure 8, the turbidity values can be normalized with respect to N_0, the initial molar concentration of seed protein molecules, and the time scale can be nondimensionalized according to

$$t^* = \beta N_0 t \tag{31}$$

The values of N_0 for a given initial concentration of ligand C_B° and of protein C_A° are calculated from eq 13 and 16 using the binding equilibrium constant K_{eq} obtained from the Scatchard plot (Figure 5). Equation 31 can be rearranged to solve for β, the kinetic parameter characterizing the precipitation process:

$$\beta = \frac{t_{1/2}^*}{N_0 t_{1/2}} \tag{32}$$

where $t_{1/2}$ denotes the time determined experimentally for the normalized turbidity $\tau/N_A N_0$ to achieve half of its final long-time value and $t_{1/2}$* denotes the value of the dimensionless time at which the Mie theory predicts a normalized turbidity $\tau/N_A N_0$ equal to half of the long-time value. It was observed that by normalizing the experimental turbidity values at long time (equilibrium) with respect to the number density of precipitable protein molecules, the values of $\tau/N_A N_0$ all approached a common value of approximately 15 absorbance units·Å^2/particle. (Note that the units on τ are absorbance units per unit path length.) The normalized turbidity predicted by the Smoluchowski–Mie theory is very sensitive to the value of ϵ, the volume fraction of solvent in the protein precipitates, and to the value of b_∞, the value of b at long time. With smaller values of ϵ, the calculated turbidity at a given value of b is larger because the refractive index difference between protein precipitate and solvent is greater. For each value of ϵ, the value of b_∞ was chosen such that the normalized turbidity approached 15 absorbance units·Å^2/particle at long time. The corresponding values of ϵ and b_∞ are collected in Table III. With each set of ϵ, b_∞ values, the Smoluchowski–Mie theory predicts a different dimensionless time $t_{1/2}$* at which the normalized turbidity achieves half of its final value. These values are also shown in Table III. With the values of $t_{1/2}$* now determined, the experimental time scales can now be nondimensionalized by measuring $t_{1/2}$ experimentally and combining eqs 31 and 32 to obtain

$$t^* = \frac{t_{1/2}^*}{t_{1/2}} t \tag{33}$$

The values of N_0 and $t_{1/2}$ for each ratio of initial ligand concentration C_B° to initial protein concentration C_A° used in the precipitation experiments (Figure 8) are shown in Table IV. The specific dependence of β and N_0/C_A° on the molar ratio C_B°/C_A° is shown in Figure 11 for the case of ϵ equal to 0.9. The values of β differ from those at other values of ϵ due to the dependence of β on $t_{1/2}$* (see eq 32). However, the range of values of β shown in Figure 11 (10 000–70 000 M^{-1} s^{-1}) is typical. They are seen to be somewhat larger than the forward rate constant k for binding of DMPE-B in $C_{12}E_8$ micelles to avidin (2000 M^{-1} s^{-1}). It is not possible that affinity precipitation can occur without first binding DMPE-B ligand to the protein. Thus, the rate constant k must depend on the size of the surfactant aggregate in which the ligand is solubilized and with $C_{12}E_8$ concentrations at or *below* the CMC, k must be larger than 2000 M^{-1} s^{-1}. The comparison between the Smoluchowski–Mie theory and the experimental normalized turbidity data is illustrated in Figure 12. The overall agreement is good, particularly for short times. At longer times, the theory overpredicts the turbidity. This may be attributable to the artificial truncation of the size distribution at b_∞. In reality, the particle size distribution achieves a maximum possible aggregate size which is dictated by a balance of growth due to agglomeration and break-up due to shear forces. These forces which give rise to break-up of agglomerates begin to become important for particle sizes smaller than the maximum possible. Thus, one might expect the experimental turbidity to fall below the theory at long times. Nonetheless, the agreement between theory and experiment in Figure 12 and the universal character of the rescaled experimental data suggest that the theory correctly captures the essential physical elements of the precipitation phenomenon.

Table IV. Values of Initial Seed Particle Concentration N_0 and of Experimental Half-Time $t_{1/2}$ as a Function of Initial DMPE-B Concentration for Avidin (1 μM) Affinity Precipitation Experiments (Figure 8)

DMPE-B conn (μM)	N_0 (μM)	$t_{1/2}$ (s)	DMPE-B conn (μM)	N_0 (μM)	$t_{1/2}$ (s)
1	0.139	1260	5	0.960	468
2	0.412	920	6	0.982	260
2.5	0.549	765	10	0.993	149
4	0.895	501	18.75	0.999	109

Modeling of QLS Diameter of Protein Aggregates. The theory developed have for the precipitation kinetics and the turbidity of precipitating protein mixture can also be used to predict the size of the protein aggregates that would be measured from a QLS experiment. For a polydisperse population of scattering particles, QLS measures an average diffusivity weighted by the concentration and the square of the molecular weight (Berne and Pecora, 1976):

$$\langle D \rangle = \frac{\int_1^\infty C_{(A^*)_n} M_n^2 D_n \, dn}{\int_1^\infty C_{(A^*)_n} M_n^2 \, dn} \tag{34}$$

In eq 34, M_n denotes the molecular weight of a protein aggregate containing n protein molecules, D_n denotes the diffusion coefficient of that protein aggregate, and $C_{(A^*)_n}$ is the concentration of that aggregate given by eq 19. The diffusion coefficient D_n depends on the aggregation number n through the aggregate radius n and the Stokes–Einstein equation:

$$D_n = \frac{k_B T}{6\pi\eta a_n} \tag{35}$$

where a_n is given by eq 28. The molecular weight of a protein aggregate is given by

$$M_n = nM_1 + \frac{4}{3}\epsilon\rho_w \pi a_n^3 \tag{36}$$

where ρ_w is the density of water. Combining eqs 19, 28, and 34–36, and using Stirling's approximation for large n,

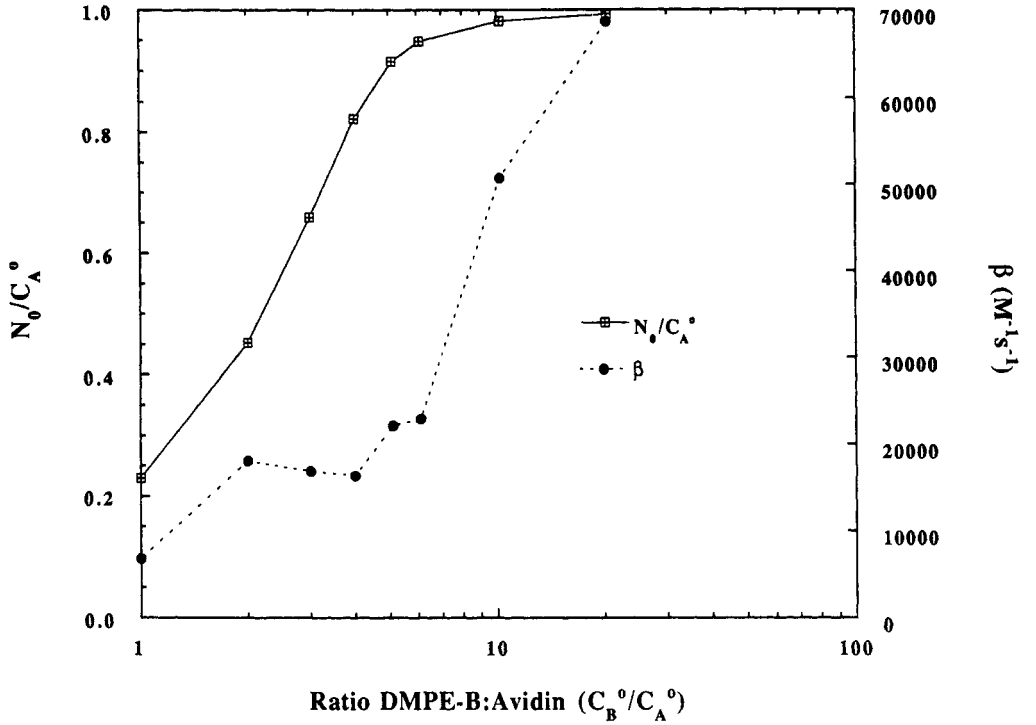

Figure 11. Dependence of N_0/C_A° and kinetic parameter β on molar ratio of ligand to protein concentration (C_B°/C_A°) for $\epsilon = 0.9$.

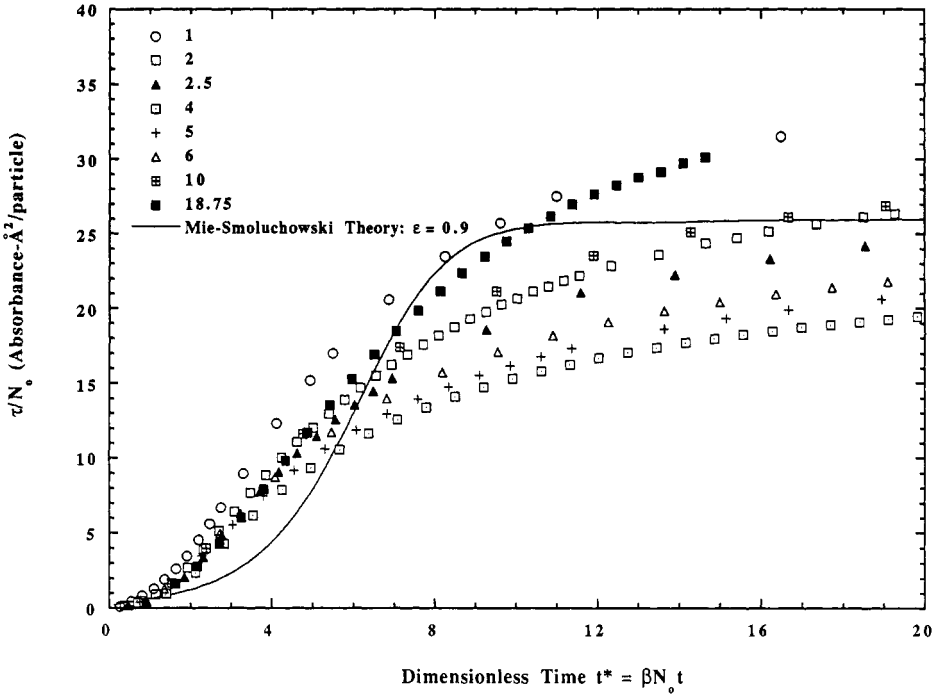

Figure 12. Dependence of normalized turbidity $\tau/N_A N_0$ on dimensionless time t^* according to the Smoluchowski–Mie theory (solid lines) and the experiment (data points). Data points correspond to the mole ratios of DMPE-B to avidin as noted in Figure 8.

the following expression is obtained for the mean particle diameter as measured by a QLS experiment:

$$\langle 2a_n \rangle = \frac{2a_1 \int_1^\infty e^{-\mu n} n^{1/2}\, dn}{(1-\epsilon)^{1/3} \int_1^\infty e^{-\mu n} n^{1/6}\, dn} \qquad (37)$$

The quantity μ is given by eq 30. Equation 37 allows for the prediction of protein precipitate particle diameter as measured by QLS. Using the same experimental variables in Table II and values of ϵ and b_∞ as used in the fit of normalized turbidity (Figure 12), eq 37 predicts a growth in particle size as measured as QLS versus dimensionless time t^* as shown in Figure 13. These predictions are compared with an experiment in which C_A° was 0.5 μM, C_B° was 1.9 μM, and the $C_{12}E_8$ concentration was 75 μM. The time scale was made dimensionless using eq 33, values of $t_{1/2}^*$ corresponding to ϵ values of 0.9 and 0.95, and an experimental $t_{1/2}$ value corresponding to a ligand-to-protein mole ratio of 3.8. The predictions of the Smoluchowski theory (eq 37) for the two different ϵ values of 0.9 and 0.95 are seen to bracket the experimental data. Thus, a very acceptable simultaneous fit of experimental turbidimetric data and quasielastic light scattering data can be obtained from the Smoluchowki–Mie theories using a

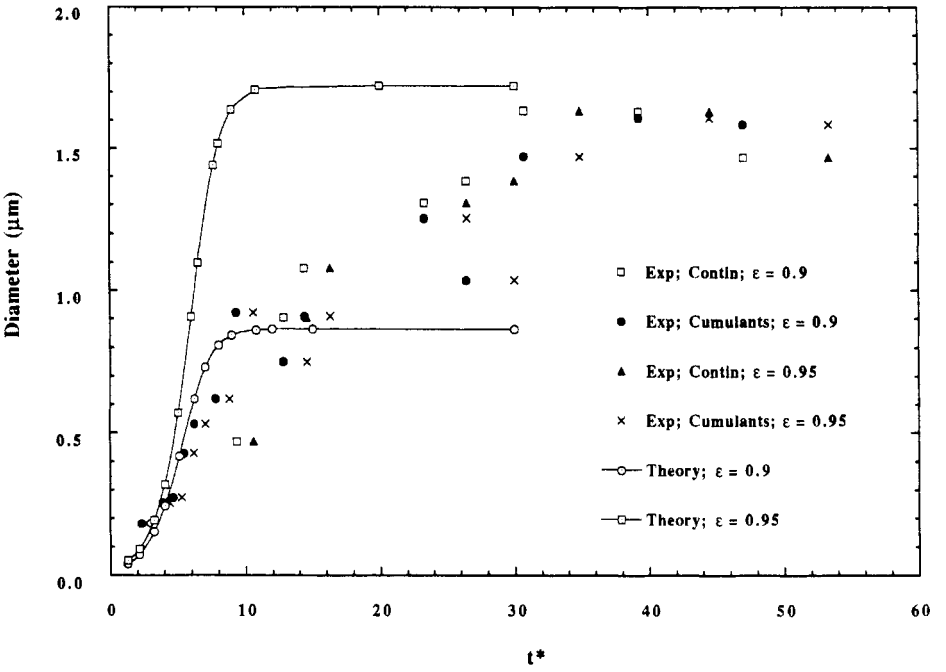

Figure 13. Diameter of protein aggregates as measured by QLS versus dimensionless time t^*. Experimental measurements of average diameter by quasielastic light scattering versus dimensionless time t^* for a precipitation experiment in which the initial avidin concentration was 0.5 μM, the initial DMPE-B concentration was 1.9 μM, and the $C_{12}E_8$ concentration was 75 μM. In nondimensionalizing the time axis, N_0 was calculated to be 0.395 μM and β was taken to be 14 200 M^{-1} s^{-1}. The theoretical predictions of diameter versus t^* were performed for ϵ values of both 0.9 and 0.95.

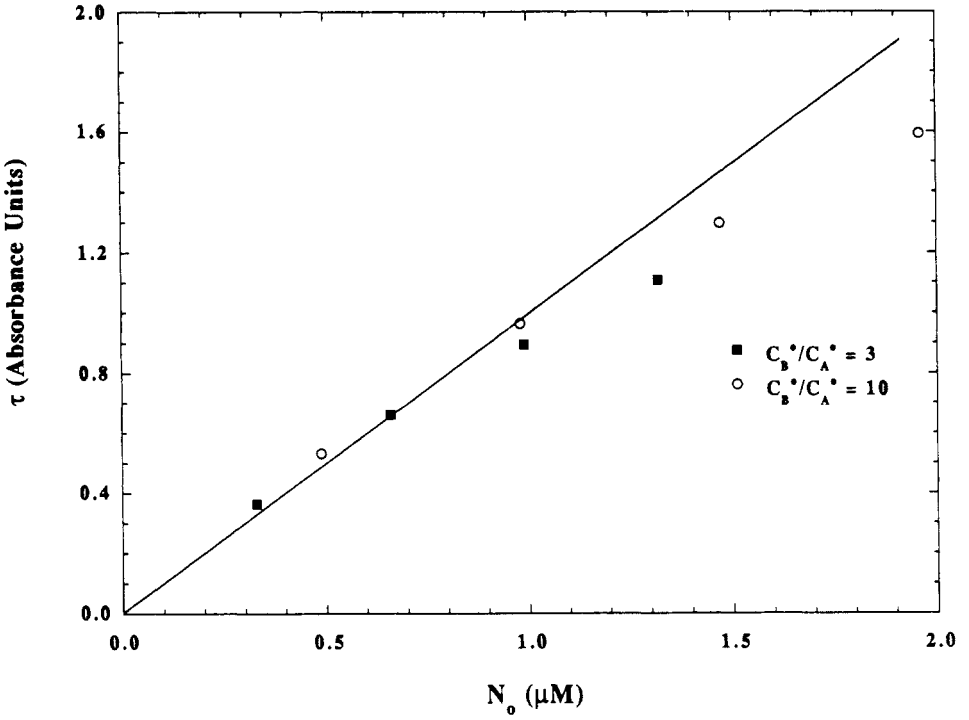

Figure 14. Long-time turbidity of solutions undergoing affinity precipitation in which the initial avidin concentration is varied. The abscissa corresponds to calculated values (eqs 11 and 19) of N_0 in which the initial avidin concentration C_A° is varied from 0.5 to 2.0 μM and the ratio of initial DMPE-B concentration to initial avidin concentration C_B°/C_A° was either 3 (solid squares) or 10 (open circles). The solid straight line represents a prediction of the Mie–Smolcuhoski theory which is forced to pass through the data corresponding to C_A° = 1 μM.

solvent volume fraction ϵ in the range of 0.9–0.95, a b_∞ value of 0.99697–0.99847, and kinetic parameter β which is a unique function of the ratio C_B°/C_A° (see Figure 11).

Yield of Affinity Precipitation. In addition to turbidity and QLS particle size, the yield of the affinity precipitation was also measured by monitoring the absorbance at 280 nm of the 1 μM avidin solution before and after adding DMPE-B in submicellar $C_{12}E_8$ solutions. This experiment was performed at molar ratios of DMPE-B to avidin of 2, 4, and 6. The resulting yields (i.e., the percentage of protein which precipitated and which ultimately sedimented from solution) were determined to be 32, 81, and 76%, respectively, for the three molar ratios. The yield of the precipitation reaction can also be calculated from the Smoluchowski theory. Presumably, there is a broad distribution of particle sizes and corresponding aggregation

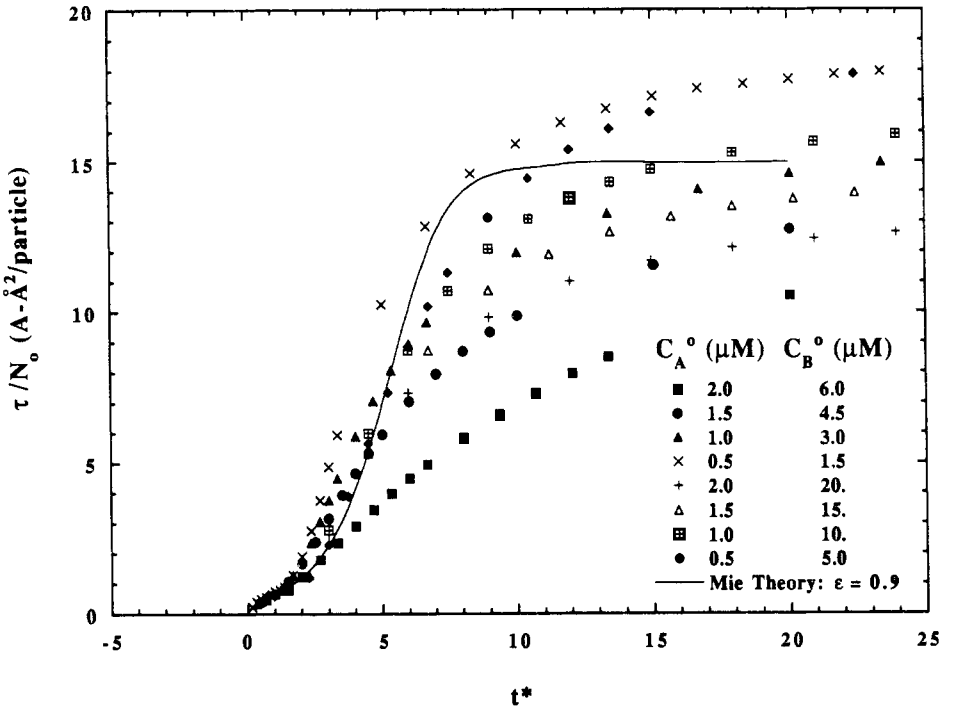

Figure 15. Comparison of the Smoluchowski–Mie theory and experiment for kinetics of affinity precipitation. The solid line denotes the prediction of the Smoluchowski–Mie theory of kinetics of affinity precipitation with solvent volume fraction ϵ of 0.9. Data points represent experiments performed over a range of $C_A°$ (0.5–2.0 μM) and $C_B°$ (1.5–20 μM). The time axis was made dimensionless by eq 34 using $N_o = 0.66C_A°$ and $\beta = 16\,000$ M^{-1} s^{-1} for experiments in which $C_B°/C_A° = 3$ and $N_o = 0.98C_A°$ and $\beta = 51\,000$ M^{-1} s^{-1} for experiments in which $C_B°/C_A° = 10$.

numbers following the onset of precipitation. There will be some cutoff value of aggregation number n_{min} below which the aggregates are still sufficiently small to be Brownian. Particles larger than this cutoff size will ultimately sediment. The yield is related to this cutoff aggregation number through

$$\text{yield} = \frac{\int_{n_{min}}^{\infty} nC_{(A^*)_n}\,dn}{N_o} \tag{38}$$

In eq 38, the concentration of aggregates with n protein molecules $C_{(A^*)_n}$ is calculated from eq 19. The value of n_{min} was fit to eq 38 at the DMPE-B to avidin mole ratio of 2, for which the yield was 32%. The value of n_{min} obtained this way was 800, which corresponds to an aggregate diameter of 880 Å. This value of n_{min} was then used to predict the yield at the other mole ratios. The yield predicted at $C_B°/C_A° = 4$ is 58% while at $C_B°/C_A° = 6$ it is predicted to be 70%. These values are in fair agreement with the experimental values of 81 and 76%, respectively. They lend further support to the notion that the Smoluchowski theory captures much of the physics of the observed precipitation phenomenon.

Effect of Initial Avidin Concentration on Turbidity and Kinetics of Affinity Precipitation. In order to test the predictions of the Smoluchowski–Mie theory at conditions of affinity precipitation other than those used to fit the kinetic parameters, precipitation experiments were performed at varying initial avidin concentration. The Smoluchowski–Mie theory predicts that the long-time value of the turbidity should be directly proportional to N_o, the initial concentration of precipitable protein monomers (see eq 29). Figure 14 presents values of turbidity at long times versus N_o for affinity precipitation experiments in which the initial avidin concentration was varied from 0.5 to 2.0 μM. The solid line is a straight line which passes through the origin and through the data points corresponding to initial avidin concentrations of 1 μM (for which the kinetic parameters of Table IV were fit). The linearity of τ with N_o is reasonably well obeyed, although there is some disagreement at the higher N_o values for which the experimental data fall some 15–20% below those values predicted by the straight line. The agreement between the predictions of the Smoluchowski–Mie theory and the experimental data on the *kinetics* of affinity precipitation were also compared. Figure 15 presents data on the dependence of normalized turbidity τ/N_AN_o on dimensionless time t^* in a series of experiments in which the initial avidin concentration was varied from 0.5 to 2.0 μM, the initial DMPE-B concentration was varied from 1.5 to 20 μM, and the $C_{12}E_8$ concentration was 75 μM. The value of N_o was calculated from eqs 8 and 17 and was determined to be $0.66C_A°$ for those experiments in which $C_B°/C_A° = 3$ and was determined to be $0.98C_A°$ for those experiments in which $C_B°/C_A° = 10$. The kinetic parameter β was assumed to be a function only of the ratio of initial ligand concentration to initial avidin concentration ($C_B°/C_A°$) (see Figure 12). With a volume fraction of solvent ϵ equal to 0.9, the value of β thus calculated was 16 000 M^{-1} s^{-1} for those experiments in which $C_B°/C_A° = 3$ and was 50 800 M^{-1} s^{-1} for those experiments in which $C_B°/C_A° = 10$. This value of ϵ is within the range of values which fits the QLS data reasonably well (see Figure 13). The agreement between theory and experiment is very good at short times ($t^* < 5$). At longer dimensionless times ($t^* > 5$), there is more spread in the experimental data about the theory, much of which is attributable to the overprediction of long-time turbidity values at the higher values of N_o as described above. Overall, however, the predictions of the theory are within the experimental values within 25% over the range of experimental values of $C_A°$, $C_B°$, and time. The Smoluchowski–Mie theory provides a useful estimate of the time course of the affinity precipitation and the ultimate turbidity values achieved.

Conclusions

Surfactant-solubilized, affinity-ligand-modified phospholipids can be employed for the affinity precipitation of proteins containing multiple binding sites. In the avidin/DMPE-B model system, the binding interaction is specific, and functionally active avidin can be obtained in high yield and purity from a model protein mixture as well as from egg white, a crude mixture of biological origin. The kinetics of the aggregation step are reasonably rapid (order of minutes) and can be increased by increasing the ligand-to-protein ratio. This parameter as well as those of surfactant and protein concentration provides a potential means for optimization of this method in a separation scheme. The progress of the aggregation is easily monitored by absorbance (turbidity) or mean particle size measurements (QLS). Precipitation can occur both above and below the CMC of the mixed phospholipid–surfactant; however, above the CMC precipitation seems to be limited to surfactant and ligand concentrations which provide at least two ligands per micelle, i.e., for which the micellar ligand is polyvalent. There is no significant coprecipitation of $C_{12}E_8$ with the protein–phospholipid aggregates. Thus, the sole function of the nonionic surfactant appears to be to solubilize the ligand-modified phospholipid, which is virtually insoluble in aqueous systems. This observation, together with the observation that precipitation occurs readily below the CMC, suggests that the mechanism for surfactant-mediated affinity precipitation involves an initial rapid binding step between the ligand-modified phospholipid and the protein followed by a slower hydrophobic interaction between the nonpolar alkyl side chains of the phospholipid that results in aggregation (see Figure 1). The kinetics of the precipitation are shown to conform well to the Smoluchowski theory using kinetic rate parameters which are linearly proportional to the number of protein molecules in each of the two aggregating species. The turbidity of the precipitating suspension is shown to be well-modeled by the Mie theory of light scattering. This theoretical framework aids in predicting the kinetics of precipitation under conditions other than those which have been determined experimentally.

Notation

a_1 radius of avidin monomer (=35 Å) (eq 28)

a_n radius of protein aggregate containing n avidin monomers and entrained solvent

a_{nm} rate constant for agglomeration of two protein aggregates, one containing n protein molecules and one containing m protein molecules (eq 18)

A avidin molecule with no bound ligand

A* precipitatable avidin molecule with at least one bound DMPE-B ligand

$(A^*)_i$ protein aggregate containing i avidin molecules

AB_i avidin molecule with i bound ligand molecules

b rescaled time variable defined by eqs 20 and 23

b_∞ long-time value of b (eq 23)

B DMPE-B ligand molecule

C_A molar concentration of avidin molecules with no bound ligand

C_A° initial molar concentration of avidin molecules with no bound ligand

$C_{(A^*)_i}$ molar concentration of protein aggregates containing i avidin molecules

C_{AB_n} molar concentration of avidin molecules with n bound ligand molecules

C_B molar concentration of ligand molecules (DMPE-B, e.g.)

C_B° initial molar concentration of ligand molecules (DMPE-B, e.g.)

D_n translational diffusion coefficient of protein aggregate containing n avidin monomers and entrained solvent

$\langle D \rangle$ diffusion coefficient of polydisperse collection of protein aggregates as measured by quasielastic light scattering (eq 34)

k forward rate constant for binding ligand to avidin molecule (eqs 2–5)

k_B Boltzmann's constant (eq 35)

k' backward rate constant for unbinding ligand to avidin molecule (eqs 2–5)

K_{eq} equilibrium constant for binding ligand to avidin molecule ($=k/k'$) (eq 11)

m_1 refractive index of protein aggregate (eq 26)

m_2 refractive index of aqueous buffer solution (eq 26)

M_1 molecular weight of avidin monomer (eq 36)

M_n molecular weight of protein aggregate containing n avidin monomers and entrained solvent (eq 34)

N total molar concentration of protein aggregates (eq 21)

N_A Avogadro's number, 6.02×10^{23} molecules/mol

N_o total concentration of protein monomer in aggregates (eqs 16 and 22)

Q_{ext} extinction coefficient in units of absorbance per unit path length corresponding to protein aggregates (eqs 24 and 25)

S equilibrium hyperchroic shift in absorbance units of ligand binding to avidin

S_{max} maximum possible hyperchroics shift for a given initial avidin concentration of ligand binding to avidin

t time

t^* dimensionless time defined by eq 31 for precipitation experiments

$t_{1/2}$ half-time in precipitation experiments, i.e., time required for turbidity to achieve half of its long-time value in a given experiment

$t_{1/2}^*$ dimensionless half-time, i.e., value of dimensionless time in Smoluchowski–Mie theory at which normalized turbidity achieves half of its long-time value

T absolute temperature

y_A dimensionless avidin concentration ($=C_A/C_A^\circ$)

y_B dimensionless ligand concentration ($=C_B/C_A^\circ$)

y_{AB_i} dimensionless concentration of avidin molecules with i bound ligands ($=C_{AB_i}/C_A^\circ$)

Greek Symbols

β kinetic parameter characterizing precipitation defined by eq 18

ϵ volume fraction of solvent (aqueous buffer) in protein aggregate

η viscosity of medium (eq 35)

λ_{vac} wavelength of incident radiation

μ defined by eq 30

ν number of bound ligand molecules per protein

ρ scattering vector defined by eq 26

ρ_w mass density of solvent (aqueous buffer)

τ total turbidity due to scattering of protein aggregates

τ_n turbidity due to scattering of protein aggregates containing n protein molecules and entrained solvent

ξ dimensionless time in ligand binding experiments defined by eq 10

Acknowledgment

We gratefully acknowledge the financial support of the National Science Foundation through Grant CTS-8904192. The yield calculations were performed by Mr. A. Singh.

Literature Cited

Adamson, A. W. *Physical Chemistry of Surface*, 4th ed.; Wiley: New York, 1982.

Bayer, E. A.; Rivnay, B.; Skutelsky, E. On the mode of liposome–cell interactions: biotin-conjugated lipids as ultrasound probes. *Biochim. Biophys. Acta* **1979**, *550*, 464–473.

Bell, D. J.; Hoare, M.; Dunnill, P. The formation of protein precipitates and their centrifugal recovery. *Adv. Biochem. Eng. Biotech.* **1983**, *26*, 1–72.

Berne, B. J.; Pecora, R. *Dynamic Light Scattering*; Wiley: New York, 1976.

Brown, W.; Pu, Z.; Rymden, R. Size and shape of nonionic amphiphile micelles: NMR self-diffusion and static and quasi-elastic light-scattering measurements on $C_{12}E_5$, $C_{12}E_7$, and $C_{12}E_8$ in aqueous solution. *J. Phys. Chem.* **1988**, *92*, 6086–6094.

Drake, R. L. A general mathematical survey of the coagulation equation. In *Topics in Current Aerosol Research*; Hidy, G. M., Brock, J. R., Eds.; Pergamon: New York, 1972; Part 2, Vol. 3, pp 202–376.

Flygare, S.; Griffin, T.; Larsson, P.-O.; Mosbach, K. Affinity precipitation of dehydrogenases. *Anal. Biochem.* **1983**, *133*, 409–416.

Gear, C. W. *Numerical Initial-Value Problems in Ordinary Differential Equations*. Prentice-Hall: Englewood Cliffs, NJ; 1971.

Green, N. M. Avidin 3. The nature of the biotin-binding site. *Biochem. J.* **1964**, *89*, 599–609.

Guzman, R. Z.; Kilpatrick, P. K.; Carbonell, R. G. Affinity precipitation of avidin using ligand-modified surfactants. *Downstream Processing and Bioseparation: Recovery and Purification of Biological Products*; Hamel, J. F., Hunter, J. B., Sikdar, S. K., Eds.; ACS Symposium Series 419; American Chemical Society: Washington, DC, 1990; pp 212–236.

IMSL Math Library. *Fortran Subroutines for Mathematical Applications*; *Version 1.0*; IMSL: Houston, TX, 1987; Section 5.1.1, Solution of the Initial Value Problem for ODEs.

Koppel, D. E. Analysis of macromolecular polydispersity in intensity correlation spectroscopy: the method of cumulants. *J. Chem. Phys.* **1972**, *57*, 4814–4820.

Larsson, P.-O.; Mosbach, K. Affinity precipitation of enzymes. *FEBS Lett.* **1979**, *98*, 333–338.

Larsson, P.-O.; Flygare, S.; Mosbach, K. Affinity precipitation of dehydrogenases. *Methods Enzymol.* **1984**, *104*, 364–369.

McCormick, D. B.; Roth, J. A. Specificity, stereochemistry, and mechanisms of the color reaction between *p*-dimethylcinnamaldehyde and biotin analogs. *Anal. Biochem.* **1970**, *34*, 226–336.

McPherson, A. Useful principles for the crystallization of proteins. In *Crystallization of Membrane Proteins*; Michel, H., Ed.; CRC Press: Boca Raton, FL, 1991; Chapter 1, pp 1–51.

Nilsson, P.-G.; Wennerstrom, H.; Lindman, B. Structure of micellar solutions of nonionic surfactants: Nuclear magnetic resonance self-diffusion and proton relaxation studies of poly(ethylene oxide) alkyl ethers. *J. Phys. Chem.* **1983**, *87*, 1377.

Pearson, J. C.; Burton, S. J.; Lowe, C. R. Affinity precipitation of lactate dehydrogenase with a triazine dye derivative: selective precipitation of rabbit muscle lactate dehydrogenase with a Procion Blue H-B analog. *Anal. Biochem.* **1986**, *158*, 382–389.

Powers, J. D.; Kilpatrick, P. K.; Carbonell, R. G. Protein purification by affinity binding to unilamellar vesicles. *Biotechnol. Bioeng.* **1989**, *33*, 1267–1276.

Provencher, S. W. A constrained regularization program for inverting data represented by linear algebraic or integral equations. *Comput. Phys. Commun.* **1982a**, *27*, 213–227.

Provencher, S. W. CONTIN: A general purpose constrained regularization program for inverting noisy algebraic and integral equations. *Comput. Phys. Commun.* **1982b**, *27*, 229–242.

Rosen, M. J.; Cohen, A. W.; Dahanayake, M.; Hua, X.-J. Relationship of structure to properties in surfactants. 10. Surface and thermodynamic properties of 2-dodecylpol(ethenoxyethanol)s, $C_{12}H_{25}(OC_2H_4)_xOH$, in aqueous solution. *J. Phys. Chem.* **1982**, *86*, 541–545.

Schneider, M.; Guillot, C.; Lamy, B. The affinity precipitation technique: Application to the isolation and purification of trypsin from bovine pancreas. *Ann. N.Y. Acad. Sci.* **1981**, *369*, 257–263.

Senstad, C.; Mattiasson, B. Affinity precipitation using chitosan as ligand carrier. *Biotechnol. Bioeng.* **1989a**, *33*, 216.

Senstad, C.; Mattiasson, B. Purification of wheat germ agglutinin using affinity flocculation with chitosan and a subsequent centrifugation or flotation step. *Biotechnol. Bioeng.* **1989b**, *34*, 387–393.

Senstad, C.; Mattiasson, B. Precipitation of soluble affinity complexes by a second affinity interaction: A model study. *Biotechnol. Appl. Biochem.* **1989c**, *11*, 41–48.

Tanford, C. *The Hydrophobic Effect*, 2nd ed.; Wiley: New York, 1980.

Taniguchi, M.; Kobayashi, M.; Natsui, K.; Fujii, M. Purification of staphylococcal protein A by affinity precipitation using a reversibly soluble-insoluble polymer with human IgG as a ligand. *J. Ferment. Bioeng.* **1989**, *68*, 32–36.

Ueno, M.; Takasawa, Y.; Miyashige, H.; Tabuta, Y.; Meguro, K. Effects of alkyl chain length on surface and micellar properties of octaethylene glycol *n*-alkyl ethers. *Colloid Polym. Sci.* **1981**, *259*, 761–766.

Van Dam, M. E.; Wuenschell, G. E.; Arnold, F. H. Metal affinity precipitation of proteins. *Biotechnol. Appl. Biochem.* **1989**, *11*, 492–502.

Van de Hulst, H. C. *Light Scattering by Small Particles*; Wiley: New York, 1957.

Van Holde, K. E. *Physical Biochemistry*; Prentice-Hall: New York, 1971.

Von Schulthess, G. K.; Benedek, G. B.; DeBlois, R. W. Measurement of the cluster size distributions for high functionality antigens cross-linked by antibody. *Macromolecules* **1980**, *13*, 939–945.

Accepted July 22, 1992.